Dorsal stream vulnerability in preterm infants – A longitudinal EEG study of visual motion perception

by

Ekaterina Zotcheva

April 2015

Developmental Neuroscience Laboratory

Department of Psychology

Norwegian University of Science and Technology

Trondheim, Norway

This Master's thesis will be submitted in approximately its present form to an international journal in the near future.

Table of contents

Acknowledgements

I am very grateful for being given the opportunity of carrying out my master's research at the Developmental Neuroscience Laboratory (Nu-lab) at the Norwegian University of Science and Technology (NTNU) in Trondheim. I am immensely grateful to my supervisor Prof. Audrey van der Meer, and co-supervisor Prof. Ruud van der Weel, for their supervision and invaluable intellectual and moral support during the work with my thesis.

I would also like to thank Seth Agyei and Kenneth Vilhelmsen for their practical and technical assistance, and for answering my many questions. Special thanks go to fellow students Regine Slinning and Helene Aaltvedt, for their valuable and helpful discussions and pleasant company during my time at the lab. Further gratitude is extended to all my lecturers and fellow students during my years as a student at NTNU, and unforgettably, the parents and their infants who have participated in this study.

I am sincerely thankful to my father Sergey Zotchev, my mother Olga Sekurova, and to my sister Natalia Zotchev for believing me and supporting me through my years as a student. Last, but not least, I owe much gratitude to Kristoffer Knutshaug, for his moral support, love, and coffee.

Trondheim, April 2015

Ekaterina Zotcheva

Abstract

High-density electroencephalogram (EEG) was used to longitudinally investigate evoked and induced brain electrical activity as a function of visual motion in full-term and preterm infants at 4-5 and 12 months of age. The infants were presented with two visual motion paradigms, optic flow and looming. The optic flow experiment simulated structured forwards and reversed optic flow and random visual motion, while the looming experiment simulated a looming object approaching on a direct collision course under three different accelerations. Analyses of visual evoked potentials (VEPs) and temporal spectral evolution (TSE) were performed on EEG data recorded with a 128-channel Geodesic Sensor Net 200 (GSN). VEP results for optic flow revealed a significant decrease in latencies for forwards and reversed optic flow, but not for random visual motion, in full-term infants with age. In addition, the 12-month-old full-term infants significantly differentiated between structured optic flow and random visual motion, with longest latencies for random visual motion, and shortest latencies for forwards optic flow. VEP results for looming revealed a significant decrease in time-to-collision of their looming-related VEP responses in the full-term infants with age. In addition, the 12-month-old full-term infants responded at a fixed time-to-collision, irrespective of loom speed. The TSE analyses revealed an increase in late alpha and early beta band synchronization in the TSE maps of the visual motion conditions in full-term infants with age. Although some preterm infants showed a similar increase in higher-frequency synchronization with age, this increase was less prominent, and some preterm infants did not show an increase at all. In addition, the preterm infants did not show a significant decrease in VEP latencies for optic flow, did not significantly differentiate between structured optic flow and random visual motion, did not show a significant decrease in time-to-collision of their looming-related VEP responses, and did not show their looming-related VEP responses at a fixed time-to-collision at 12 months of age. It was suggested that the full-term infants' progression in visual motion processing can be attributed to an increase in self-produced locomotor experience and accompanying neural maturation. The preterm infants' poorer performance on the visual motion experiments can be related to a deficit in the processing of visual motion, a dorsal stream function. More follow-up research is needed to further investigate whether the dorsal stream impairment persists into later life, and to what extent this impairment may affect the everyday lives of individuals born prematurely.

1. Introduction

When we navigate through the environment, we continuously gather perceptual information about our surroundings enabling us to make precise calculations in order to plan our next movement. Gibson (1986) suggested that perception and behavior are mutually dependent and cannot be treated separately, as our behavior is guided by what we perceive in our surroundings, while what we perceive in turn is guided by our behavior. Thus, being able to gather correct information about our movement through the environment, and being able to respond to changes, is essential to avoid accidents and missteps.

Gibson (1986) argued that changes in the *optic array* produced by the locomotion of an observer are essential for visual perception, as they provide crucial information about the locomotion itself. When an observer moves through his or her surroundings, the movements are accompanied by a flow in the optic array. This is referred to as *optic flow*, and thus describes the stream of visual information we receive about our self-motion while navigating through the surrounding environment (Bruce, Green, & Georgeson, 2003). Perception of optic flow has been proven essential in the control of walking direction (Warren, Kay, Zosh, Duchon, & Sahuc, 2001; Bruggeman, Zosh, & Warren, 2007), postural adjustment, time-to-collision calculations (Van der Meer, Van der Weel, & Lee, 1994; Kayed & Van der Meer, 2009), as well as in obstacle avoidance (Wilkie & Wann, 2003).

In addition to being able to perceive and process self-motion, it is crucial for humans, amongst many other species, to be able to perceive the approach of moving objects so as to time an appropriate response. Problems with doing so can possibly lead to collisions, as well as impair actions such as catching, ducking and kicking. Thus, the development of the ability to process visual motion, both as a result of self-motion and as a result of object motion, can be considered a very important aspect of the overall development of vision in infancy.

Developmental studies have investigated the development of timing strategies and prospective control in infants. Prospective control is our ability to make and plan precisely-timed movements which must be continuously adapted to the constantly changing environment and body (Adolph, Eppler, Marin, Weise, & Clearfield, 2000). Even highly automatized, repetitive movements such as walking must be constantly modified to suit the current demands of the context in which the movements take place (Adolph et al., 2000). Without sufficient prospective control, individuals may experience problems when responding to changes in the environment, possibly leading to injuries and difficulties while performing everyday tasks.

By simulating a looming object on a direct collision course towards the participant, researchers can investigate how the brain processes information of an imminent collision, and thus observe what timing strategy the participant uses, and whether the participant has developed sufficient prospective control so as to be able to correctly time their response to the collision (Van der Meer, Svantesson, & Van der Weel, 2012). The term "looming" refers to the last part of the optical event where an object is accelerating toward the individual (Kayed & Van der Meer, 2007). The perception of looming has been investigated in a number of different species, including pigeons (Sun & Frost, 1998), locusts (Rind & Simmons, 1997), monkeys (King & Cowey, 1992), as well as humans (Yonas, Pettersen, & Lockman, 1979; Yonas, 1981; Kayed & Van der Meer, 2000, 2007; Van der Meer et al., 2012). Pigeon studies indicate that a subpopulation of neurons in the nucleus rotundus responds selectively to objects moving on a collision course towards the bird (Wang & Frost, 1992), and that this subpopulation is divided into three groups of neurons, *tau*, *rho*, and *eta* (Sun & Frost, 1998). Tau neurons signal relative rate of expansion initiating their responses at a fixed time-to-contact, rho neurons signal absolute rate of expansion, while eta neurons signal angular size (Sun & Frost, 1998).

Yonas et al. (1979) and Náñez (1988) reported that infants respond to looming with blinks and backward head movements as early as at 3 to 6 weeks, indicating that infants exhibit sensitivity to information of an impending collision very early in development. Blinking is considered to be the best indicator of awareness to stimuli on a direct collision course in early infancy (Yonas, 1981). Correctly timing the defensive blink is essential, as blinking too early may lead to reopening of the eyes prior to the collision, while blinking too late may lead to the object hitting the eyes, possibly damaging the sensitive cornea of the eyes.

Kayed, Farstad and Van der Meer (2008) investigated preterm infants' development in their use of timing strategies when making a defensive blink to a looming object on a direct collision course. The results of this study indicate that preterm infants, when tested corrected for prematurity, follow the same developmental pattern as full-term infants, but not when tested uncorrected for prematurity. In addition, one of the preterm infants tested did not show the same switch in timing strategies as the other infants, and continued to use a less effective timing strategy when timing his defensive blink. Using a less effective timing strategy can be a sign of perceptuo-motor problems, and the same infant showed severe timing problems in a later longitudinal study of prospective control in catching (Kayed & Van der Meer, 2009).

Infants born preterm have been found to be more at risk of neurological deficits and developmental disorders. An infant is defined preterm when he/she is born before 37 completed weeks of gestation. In Norway, approximately 5.6% of infants were born preterm in 2013 (Store Medisinske Leksikon, 2014), but due to improved intensive care facilities, the chances of survival have increased greatly during the last couple of decades (Markestad & Halvorsen, 2007). A study by Jongmans, Mercuri, De Vries, Dubowitz, and Henderson (1997), showed that children born preterm are at a higher risk of having neurological and perceptuo-motor problems. In their study, the children with the lowest birth weight and the lowest gestational age were the most affected at 6 years of age in their neurological and perceptuo-motor development (Jongmans et al., 1997). Larroque et al. (2008) found that cerebral palsy, visual deficiency, and hearing deficiency frequencies decreased with increasing gestational age (Larroque et al., 2008). It has also been reported that children born very preterm have particular problems processing complex information that needs logical reasoning and spatial orientation abilities (Larroque et al., 2008). In addition, individuals born very preterm have been found to score significantly lower than individuals born full-term on motor, behavioral, and cognitive measures, and are more likely to be diagnosed with ADHD (Foulder-Hughes & Cooke, 2003). The minor motor impairments found in very-low-birthweight children have been shown to have an impact on overall school performance, despite intelligence within the normal range (Foulder-Hughes & Cooke, 2003).

At birth, the human brain is equipped with 100 billion neurons, few of which are connected. During the first years of life, millions of connections are made through an interplay of life experience and maturation, forming complex networks of neurons specialized to rapidly process different kinds of information. However, there are indications that preterm birth affects brain development. In a magnetic resonance imaging (MRI) study of brain growth from 23 to 48 weeks of gestation carried out in 113 extremely preterm infants, Kapellou et al. (2006) found that preterm infants demonstrate slower cortical growth with decreased gestational age at birth. In a MRI study of very low birthweight (VLBW) adolescents, significant cortical thinning was observed in the parietal and temporal lobe in the VLBW adolescents when compared to a full-term control group, and observed differences between the VLBW and control group decreased with increasing gestational age (Martinussen et al., 2005). Abnormal brain volume as a result of prematurity has also been found in a MRI study by Nosarti et al. (2002), who found decreased whole brain volume, cortical grey matter

volume, and right and left hippocampal volumes in 15-year-old adolescents born very preterm.

In healthy full-term infants, the fiber volume of white matter increases during early infancy until adulthood due to ongoing axonal myelination (Paus et al., 2001; Mukherjee et al., 2002; Dubois, Hertz-Pannier, Dehaene-Lambertz, Cointepas, & Le Bihan, 2006), which serves to increase the speed of neural communication. Hüppi et al. (1998) found that preterm infants have less cortical white matter at 2 weeks of life compared to full-term controls, a finding confirmed by a later MRI study (Mewes et al., 2006), showing that preterm infants at 2 weeks of life corrected for prematurity had less unmyelinated and myelinated white matter compared to full-term controls. These results seem to persist into later childhood and adolescence. In a diffusion tensor imaging (DTI) study, Counsell et al. (2008) showed that preterm children at two years of age corrected for prematurity showed abnormalities in regions of cerebral white matter measured by fractional anisotropy (FA), which is thought to reflect fiber density, axonal diameter and myelination. A DTI study of VLBW adolescents revealed significantly lower FA values in seven out of thirteen white matter areas in the VLBW group compared to the control group (Skranes et al., 2007). FA values were significantly correlated with overall scores on Griffiths Mental Developmental Scales and eye-hand coordination sub-scores in preterm infants at two years of age (Counsell et al., 2008), and with visual motor and visual perceptual tests, IQ, and Grooved Pegboard score in VLBW adolescents (Skranes et al., 2007), indicating that abnormal cerebral white matter in preterm infants may be an explanation as to why individuals born preterm more often show neurodevelopmental impairments.

Visual information is believed to be processed through two separate, yet interacting, cortical streams. The ventral stream, often referred to as the "what" stream or as the parvocellular visual pathway, is responsible for object recognition, and leads from the occipital lobe to the temporal lobe. The dorsal stream, often referred to as the "where" stream or as the magnocellular visual pathway, is essential in attention, decision making, motion perception, and movement planning, and leads from the primary visual cortex to the medial temporal (MT) and medial superior temporal (MST) areas, together known as V5/MT+ (Morrone et al., 2000; Smith, Wall, Williams, & Singh, 2006), and on to the parietal lobe (Andersen, 1997).

Newborns can track a horizontally moving object (Haith, 1966); indicating that motion perception is present already at birth. The development of motion perception continues

through childhood and is well established by age 12 (Parrish, Giaschi, Boden, & Dougherty, 2005). Deficits in visual motion perception, which is a dorsal stream function, have been observed in a number of developmental disorders such as autism spectrum disorders (Spencer et al., 2000), developmental dyslexia, developmental dyspraxia, Williams syndrome, and Fragile X syndrome (Braddick, Atkinson, & Wattam-Bell, 2003; Grinter, Maybery, & Badcock, 2010). Grinter et al. (2010) suggest that a dorsal stream vulnerability in developmental disorders may stem from a loss of magnocellular (M) cells in the dorsal stream arising from a general disease-related neuron loss. Studies of preterm children without cerebral palsy have found deficits in visuomotor skills, indicating impaired dorsal stream functioning (Van Braeckel et al., 2008). Guzzetta et al. (2009) found that preterm infants, irrespective of the presence of brain damage, show impaired dorsal stream-related functions compared to full-term controls. These findings suggest that dorsal stream vulnerability may not be restricted to developmental disabilities, but that it may also be a result of preterm birth, and that such a vulnerability can be detected already at infancy.

Research has pinpointed the processing of complex visual motion in the human brain to the V5/Medial Temporal (MT) area and the Medial Superior Temporal (MST) area, together known as MT+ (Morrone et al., 2000; Smith et al., 2006), and to areas of the dorsal visual stream, which have been found to have neurons selectively activated by motion stimuli (De Jong, Shipp, Skidmore, Frackowiak, & Zeki, 1994). Increased attention has been given to the use of non-invasive electroencephalogram (EEG) recordings to study the neural basis of motion perception at the millisecond time scale (Van der Meer, Fallet & Van der Weel, 2008). Visual evoked potentials (VEPs), a term used to describe event-related potentials (ERPs) elicited by visual stimuli (Luck, 2005), measured by EEG have proven to be applicable in studying the neural basis of motion perception at the millisecond time scale (Van der Meer et al., 2008). In EEG, motion VEPs are dominated by a negativity around 150-200 ms, which has been suggested to have its origin in area MT+ (Probst, Plendl, Paulus, Wist, & Scherg, 1993).

Using magnetoencephalography (MEG) recordings in adults, Holliday and Meese (2005) found differences in VEPs relative to the motion stimulus presented. Gilmore, Hou, Pettet, and Norcia (2007) also found an asymmetry in responses to different optic flow stimuli in adults. Research suggests differential sensitivity of the visual cortex to different classes and speeds of optic flow and motion-defined figure patterns (Fesi, Thomas, & Gilmore, 2014). EEG studies measuring VEPs have shown that optic flow is processed more rapidly than

random visual motion, possibly because humans have more experience with optic flow in their everyday lives (Van der Meer et al., 2008; Agyei, Holth, Van der Weel, & Van der Meer, 2014). Van der Meer et al. (2008) found that infants who have not yet started to walk process optic flow slower, and that processing time decreases with increased experience with flow due to self-initiated navigation through the environment (e.g. walking). This finding was also confirmed in a later study by Agyei et al. (2014) showing that infants' processing time of optic flow decreased from 3-4 to 11-12 months of age, a finding that can be attributed to increased experience with self-initiated locomotion. Thus, a progression showing faster processing of visual information with increasing age is expected in normally developing infants, especially after the onset of self-produced locomotion (Gilmore & Rettke, 2003; Gilmore, Baker, & Grobman, 2004). However, Guzzetta et al. (2009) found that preterm children (mean age = 10.7 years) without brain damage had significantly lower sensitivity to optic flow stimuli than full-term controls, a finding that supports the notion of a dorsal stream impairment in individuals born prematurely.

EEG studies have also proven to be useful in studying brain electrical activity as a function of looming stimuli. Van der Meer et al. (2012) studied looming in infants longitudinally using high-density EEG, where they observed differences in looming-related VEPs between infants when they were 5-6 months and 12-13 months of age. With age, a decrease in the time-to-collision of the looming-related VEP and VEP duration was observed, in addition to a shift from a less efficient to a more efficient timing strategy, indicating that infants' prediction of an object's time-to-collision improves with age and increased locomotor experience (Van der Meer et al., 2012).

In conjunction with the use of VEPs, growing attention has been given to EEG studies in the time-frequency domain. Van der Meer et al. (2008) reported theta-band event-related desynchronization (ERD) in 8-month-old infants when presented with optic flow stimuli compared to a static dot pattern, where they found theta-band event-related synchronization (ERS). In the same study, beta-band ERS was reported for adults when presented with motion stimuli compared to a static dot pattern, where beta-band ERD was reported (Van der Meer et al., 2008). Van der Weel and Van der Meer (2009) found that infants' induced brain activity when viewing a looming stimulus approaching under three different accelerations was dominated by theta oscillations. Agyei et al. (2014) found that with age, infants show an increase in alpha-band ERS, indicating a progression towards more adult-like visual motion processing in the brain. Lower-band frequencies such as theta-band may indicate a larger

amount of coherently activated neurons compared to higher-band frequencies such as beta-band (Pfurtscheller & Lopes da Silva, 1999). The frequency differences between infants and adults could thus be attributed to the maturational process where the infants' brains have not yet formed specialized and effective neuronal networks (Edelman, 1993; Johnson, 2000).

The present study aimed to explore the development of visual motion processing in the brain during the first year of life with a focus on the effects of preterm birth. Understanding the functional development of the brain, and possible anomalies in development due to prematurity, is important in order to ensure early intervention and diagnosis of preterm infants experiencing developmental problems. Brain electrical activity in full-term and preterm infants in response to optic flow and looming visual stimuli was investigated using high-density EEG. VEP and frequency analyses were applied to the data to investigate whether there are any significant differences in brain responses to visual motion between preterm and full-term infants. In addition, individual analyses were applied in order to detect preterm infants showing especially large discrepancies in visual motion processing. A longitudinal perspective was applied by testing preterm and full-term infants at the age of 4-5 months and again at the age of 12 months. Previous research has shown that normally developing full-term infants significantly decrease their VEP latencies as a function of optic flow and become more sensitive to optic flow as opposed to random visual motion (Van der Meer et al., 2008; Agyei et al., 2014), significantly reduce the time-to-collision of their looming-related VEPs and switch to a more efficient timing strategy (Kayed et al., 2008; Van der Meer et al., 2012), and show an increase in induced alpha-band synchronized brain electrical activity (Agyei et al., 2014) with increasing age during the first year of life. Based on these findings, and research indicating impaired dorsal stream functioning in preterm infants, the preterm infants in this study were expected to show an abnormal development of visual motion processing between the ages of 4-5 and 12 months compared to full-term controls.

2. Methods

2.1 Participants

A total of 20 healthy infants, 10 full-term and 10 preterm (7 boys and 3 girls in both groups), were recruited for this study. The preterm infants were recruited with the help of the pediatrician in charge at St. Olav's University Hospital's Neonatal Intensive Care Unit in Trondheim, Norway. The full-term infants were recruited either by contacting the parents through birth announcements in the local newspaper, or by a simple snowball technique. Students and other workers in the Department of Psychology who recently had a baby were invited to participate in the study.

One of the preterm infants did not provide sufficient data during the second testing session, and was therefore excluded from the longitudinal analysis. Therefore, no matched full-term control was included for this preterm infant in order to ensure equal group sizes. The preterm infants were born at ≤ 33 weeks of gestation (mean (SD) = 31.0 (1.8), range 28.3-33.0) with an average birth weight of 1622 g (range 1000-2670, SD = 453). The full-term infants had a mean gestational age of 39.8 weeks (range 38.2-41.6, SD = 1.2) with an average birth weight of 3462 g (range 3085-4190, SD = 387). The neurological status of the infants was not known to the experimenter. Three of the preterm infants were bottom shufflers, as reported by their parents.

The testing followed a longitudinal design where the infants were tested twice, first at 4-5 months, followed by a second session where the infants were approximately 12 months of age. Preterm and full-term infants were matched according to age and sex. In order to ensure valid matching, the preterm infants' age was corrected for prematurity. For the first session, the mean age of the preterm infants was 4.8 months (range 4.4 – 5.2, SD = 0.3), while the full-term infants had a mean age of 4.4 months (range 3.2 – 6.0, SD = 0.9). For the second session, the mean age of the preterm infants was 12.3 months (range 11.5 – 13.6, SD = 0.6), while the full-term infants had a mean age of 11.5 months (range 10.8 – 12.4, SD = 0.6).

EEG recording causes no physical pain or harm to the participant. The parents gave their informed written consent prior to the experiment and were made aware that they were free to withdraw at any time before, during, or after the experiment. One of the parents was at all times situated next to the infant during the experimental testing and had the opportunity to interrupt the experiment at any time, for whatever reason. The study has been approved by the

Norwegian Regional Ethics Committee and the Norwegian Data Services for the Social Sciences.

2.2 Stimuli

Stimuli were generated with E-Prime (Psychology Software Tools), and mirror-reversed projected by an ASK M2 projector onto a wide screen (108 cm wide, 80 cm high) (see Figure 1a). The infants were presented with two different visual motion paradigms in the respective order of optic flow and looming.

a)

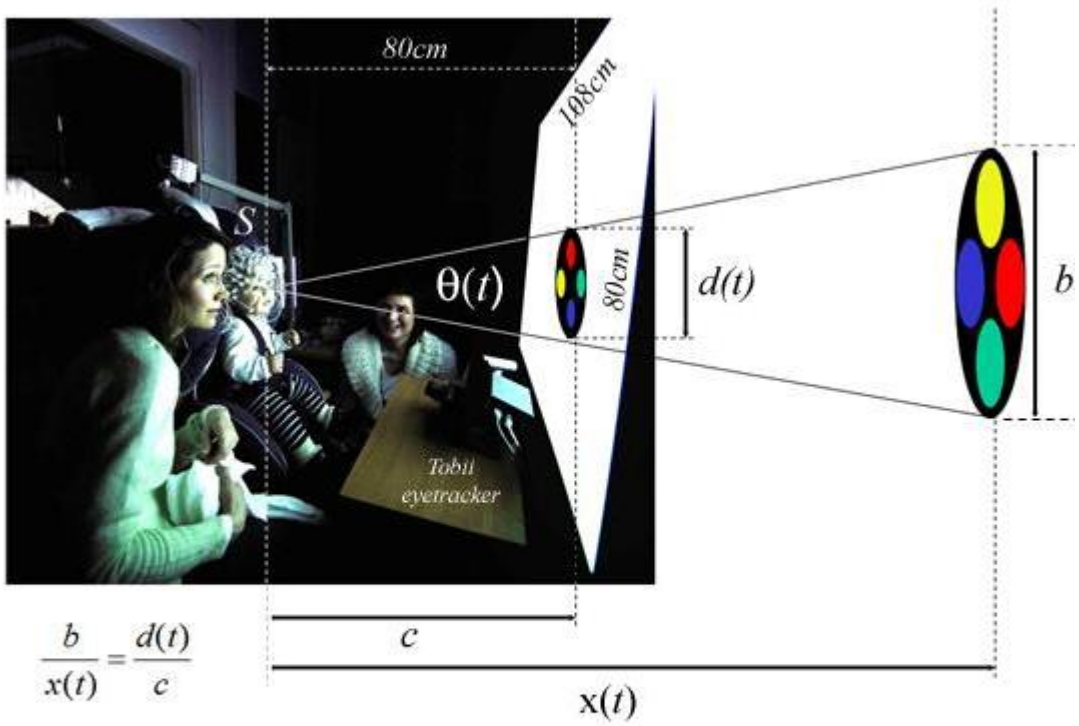

b)

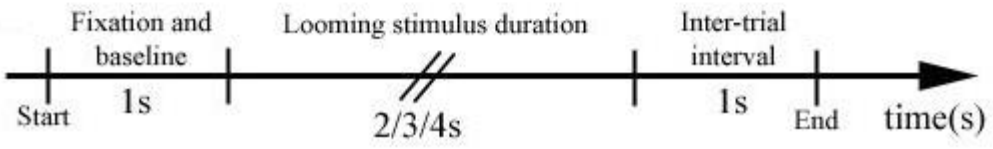

Figure 1. *Experimental setup with a diagram of the looming stimulus configuration. Same setup was used for the optic flow stimulus. a) An infant sitting in a car seat facing a wide screen on which the stimuli are projected. In the bottom left corner is a mathematical equation describing the growth of the visual loom. b) Timeline showing the approach of the looming stimuli and the time duration during the phase of fixation, looming, and inter-trial interval from start to end in a single trial.*

2.2.1 Optic flow

The optic flow stimulus consisted of 100 black randomly placed dots on a white background with a red fixation point at the center of the screen. The dots moved in different patterns, simulating three different patterns of coherent and incoherent motion: forwards optic flow, reversed optic flow, and random visual motion. In the optic flow conditions, the dots moved outward (for forwards optic flow) or inward (for reversed optic flow). In the random motion condition, the dots had the same properties as in the optic flow conditions, but moved in random directions at a constant velocity. Dots were repositioned automatically to compensate for dots moving out of the aperture. To avoid motion adaptation, a static dot pattern made up of a still optic flow pattern was used as a control condition, and was presented after each motion pattern. Duration of each motion stimulus, as well as the static dot pattern, was 1500 ms, and the different motion conditions were presented in random order. On average, each full-term participant contributed 59 (SD = 15) motion trials in each testing session, and each preterm participant contributed 51 (SD = 12) motion trials in each testing session. The trials were more or less evenly distributed across the three motion conditions.

2.2.2 Looming

The looming stimulus consisted of a black flat 2D circle with 4 different colored circles (red, green, blue, and yellow) of equal size rotating within it. The radius of the inner circles was 1/3 of the radius of the outer circle. The entire object rotated with a constant angular velocity of 300 degrees per second and was shown on a cream white background. The stimulus was programmed to loom towards the infant with different accelerations, and finally came up to the infant's face so as to create an experience of a visual collision.

The virtual object approached the infant under three different conditions with a constant acceleration over a period of 2 s (-21.1 m/s^2), 3 s (-9.4 m/s^2), and 4 s (-5.3 m/s^2). The image of the virtual object had the same size and visual angle at the beginning (diameter 6.5 cm, visual angle 5°) and the end (diameter 350 cm, visual angle 131°) of the approach, irrespective of the virtual object's approach time. At the beginning of each loom, the virtual object appeared on the screen at a virtual distance of 43.1 m, where it stayed at its minimum size for 1 s before expanding and finally disappearing, leaving the screen blank for 1 s. A reversed looming condition simulating the flat 2D circle moving away from the infant was used as a control condition in order to maintain the infant’s interest. The looming conditions,

as well as the control condition, were presented in random order. The infants were presented with an average of 46 (SD = 7) looming trials during each experimental session, not including the control condition.

2.3 Apparatus

EEG activity was recorded with a Geodesic Sensor Net 200 (GSN), which consists of an array of 128 electrodes evenly distributed across the participant's head. Onset and offset of stimuli was communicated onto the EEG-recording using E-Prime (Psychology Software Tools). As recommended for high-input-impedance EGI amplifiers by Feree, Luu, Russell, and Tucker (2001), all electrode impedances were kept under 50Ω to ensure optimal signal-to-noise ratio. The amplified EEG signals were recorded at a sampling rate of 500 Hz using Net Station software on a Macintosh computer. The recorded data were stored on a hard disk for off-line analyses.

An infrared Tobii X50 camera was used to track the infant's gaze. The visual feed was processed with Clear View software on a HP computer. In addition to the Tobii data, a digital video recorded from a camera placed in front of the infant was used off-line to monitor behavior during the experiment.

2.4 Procedure

Parents usually arrived with their infant 10 to 15 minutes prior to the experiment. At arrival, the parent(s) were informed about the experiment and consent form while the infant was given time to get acquainted with the experimental surroundings. In the process, an assistant measured the infant's head circumference for appropriate electrode net selection. The electrode net was first soaked in a solution of distilled water, saline and a few drops of baby shampoo in order to optimize electrical conductivity. The infant was seated on its parent's lap and distracted with toys while the electrode net was slightly dried off and mounted on the infant's head. Electrodes with insufficient contact with the scalp were repositioned in order to improve contact. The infant and parent were then immediately led into the experimental room.

In the experimental room, the infant was placed facing a wide screen (1.1 x 0.8 m) hanging from the ceiling 0.8 m away from the infant. The infant sat on the parent's lap during the first testing session and in a car seat with one parent right next to it during the second session. The net was plugged into an amplifier and the impedance of the electrodes was

checked. A research assistant sat beside the infant to keep him/her calm during the experimental procedure. Stimulus generation and data acquisition were managed by two assistants from the control room that was separated from the experimental room by a sound-proof window.

The experimental session began immediately after calibrating the infant's eye movements to the infrared Tobii X50 camera. The optic flow experiment was presented first, followed by the looming experiment. The infants were also presented with an occlusion experiment. Each experiment took 4-5 minutes on average. Data acquisition was carried out in one block. However, presentation of the stimuli was paused if an infant showed signs of boredom or disinterest at which time the assistant and/or parent played with the infant for a short period of time in order to revive the level of interest. The experimental session was aborted after sufficient data were acquired, or if the infant showed considerable disinterest, tiredness, or fussiness.

2.5 Data analysis

BESA (Brain Electrical Source Analysis) 6.0 software was used to carry out data analyses of the EEG raw data. Recordings were segmented with the Net Station software and exported as raw files as an initial pre-processing step. The same methods of analysis were applied to the data for both groups at both testing sessions. Bad channels and trials with artifacts caused by body/head movements were removed by visual inspection. A maximum limit of channels defined as bad was set to 10%.

For the optic flow experiment, epochs of interest around the triggers of stimulus onset were set from -200 to 800 ms. Eye movements, such as blinks and horizontal and vertical eye movements were corrected manually. Low cut-off filter was set to 1.6 Hz to remove slow drift in the data; while the high cut-off filter was set to 60 Hz. Notch filter was set to 50 Hz to remove electrical noise. Based on recommended BESA settings, all channels and trials with amplitudes higher than 200 μV, gradients higher than 75 μV/sample, and signals below 0.1 μV were left out of further analyses.

For the looming experiment, low cut-off filter was set to 1.6 Hz, notch filter was set to 50 Hz, and high cut-off filter was set at 30 Hz. High cut-off filter was set at 8 Hz during VEP peak selection. A reference-free montage showing the EEG at 27 standard electrodes was used during the analysis. There was no averaging of EEG data for the looming experiment.

During the TSE (Temporal Spectral Evolution) analysis, epochs of interest around the looming-related VEP peaks were set from -300 to 300 ms.

Oscillations in the ongoing EEG can be divided into two distinct groups: evoked and induced activity. In EEG, motion VEPs are dominated by a negativity around 150-200 ms, which has been suggested to have its origin in area MT+ (Probst et al., 1993). A VEP is defined as the post-synaptic firing pattern of neurons at a particular time in relation to a visual stimulus (Webb, Long, & Nelson, 2005). Averaging techniques are commonly used to detect evoked potentials, as they are both time- and phase-locked to the stimulus onset, and averaging thus increases the signal-to-noise ratio (Pfurtscheller & Lopes da Silva, 1999).

In addition to analyses of evoked activity, such VEPs, analyses of induced activity can be used in order to fully understand the complex brain responses following a visual motion stimulus. Induced activity is, unlike evoked activity, time-locked but not phase-locked, and averaging is therefore not a suitable method for extracting this kind of activity. Frequency analysis is seen as a more suitable method for analysis of induced activity as it detects event-related time-frequency responses that are assumed to represent local cortical neuronal interactions (Pfurtscheller & Lopes da Silva, 1999). Induced activities represent specific event-related frequency changes in the ongoing EEG activity and may be made up of either an increase or decrease in amplitudes. These frequency changes may stem from increases or decreases in synchrony of the underlying neuronal populations, and reflect changes in communication between main neurons and interneurons (Pfurtscheller & Lopes da Silva, 1999). An increase in synchrony is referred to as event-related synchronization (ERS) (Pfurtscheller, 1992), while a decrease in synchrony is referred to as event-related desynchronization (ERD) (Pfurtscheller & Aranibar, 1977). Increases in ERD magnitude have been linked to an increase of task complexity (Boiten, Sergeant, & Geuze, 1992), and ERD is seen as a characteristic of cortical areas or neural structures preparing to process sensory information (Pfurtscheller, 1992). ERS, on the other hand, is often considered as a sign of neuronal networks at a resting or deactivated state (Pfurtscheller & Lopes da Silva, 1999).

2.5.1 VEP analyses

For optic flow, individual averages for the three motion conditions (forwards and reversed optic flow, and random visual motion) in addition to the static dot pattern were computed. Individual averages were re-referenced to an artificial reference calculated from the average potentials over the scalp and interpolated to 81 standard electrodes, and were used for further VEP analyses. The individual averages were combined to create a grand average for each group and each testing session, resulting in a total of four grand averages. Earlier EEG studies have shown that VEPs arising from motion stimuli have found to be dominated by a motion-sensitive negative component, the N2 wave, occurring in adults around 130-150 ms post-stimulus (Probst et al., 1993). The N2 components of the VEP waveforms were identified and values for peak latencies were recorded and subjected to further VEP analyses.

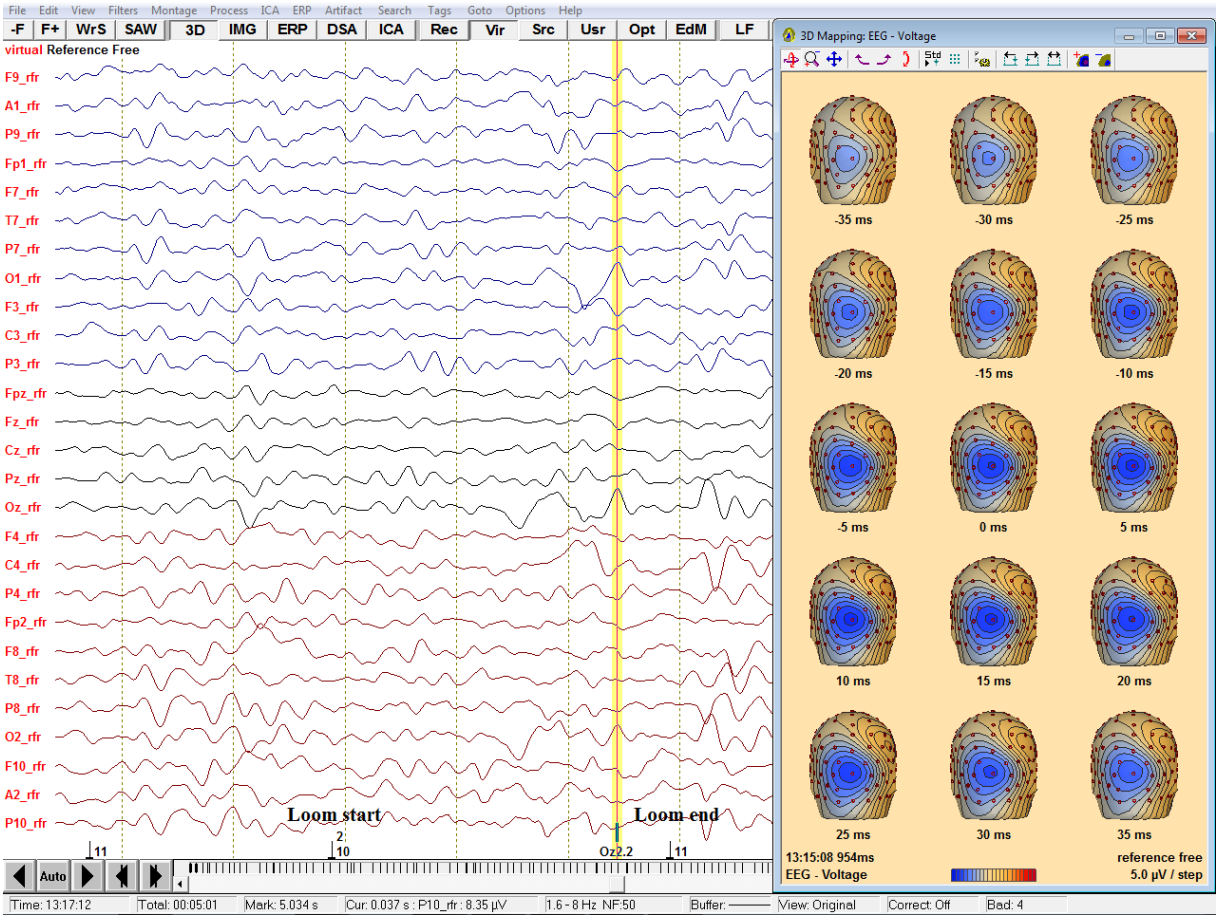

Figure 2. *EEG data analysis in BESA showing a typical looming VEP response to a 3 s loom. The VEP peak at channel Oz is marked by a yellow vertical line. The 3D-mapping in the top right corner shows a high cortical activity in the visual cortex building up over time and peaking at approximately 0.5s prior to the loom end.*

For typical looming-related VEP responses, the main occipital and parietal electrodes (Oz and Pz) were specifically observed for the three different looming conditions. Prominent VEP peaks were marked at electrode sites Oz and Pz based on earlier studies investigating the cortical sources of VEP components (Di Russo, Martínez, Sereno, Pitzalis, & Hillyard, 2002). The selected VEP peaks provided information about looming-related activity in the selected brain region. This activity could also be visualized by a 3D-mapping of a build-up and decline of voltage activity in the visual cortex on a trial-by-trial basis (see Figure 2). The criteria for selecting looming-related VEP peaks were based on the 3D-mapping procedure combined with visual inspection of peaks. All looming peaks were identified on a trial-by-trial basis. In the case of consecutive peaks in a trial, the peak closest to stimulus end showing the best cortical activity in the 3D-mapping was assumed to be more functionally related to the loom. For each VEP peak, the time remaining to stimulus end which coincided with the loom's time-to-collision was recorded.

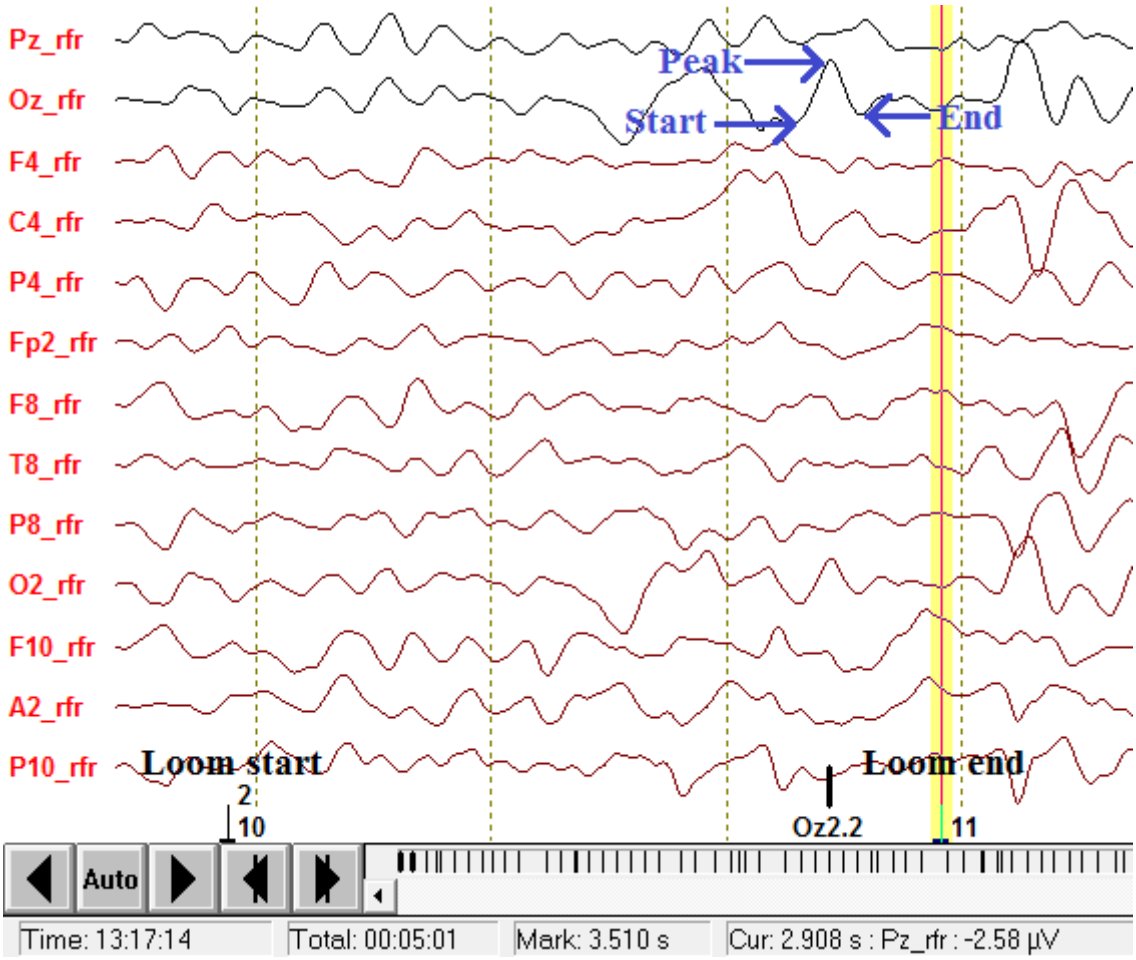

Figure 3. *Marking and timing of individual VEP in raw EEG data, showing how the start, peak and end of the looming-related VEP were manually marked in the Oz electrode of single trials.*

2.5.2 TSE analyses at the brain source space level

TSE analyses were performed in brain space using multiple source dipoles that modelled the parietal and visual cortices, which were the main brain regions of interest. There is a wide distribution of focal brain activity at the scalp due to the nature of the dipole fields and the smearing effect of the volume conduction in EEG. As a result, scalp waveforms have mixed contributions from underlying brain sources. It is therefore necessary to separate brain activity from different brain regions, which is achieved by using brain source montages derived from a multiple source model. The source model is used to create an inverse spatial filter, a source montage, which separates the different brain activities.

In analyzing the sources, a 4-shell ellipsoidal head model was created using a predefined montage optimized for analysis of visual information. The regional sources of interest were (with Talairach coordinates, Talairach & Tournoux, 1988): visual cortex lateral left (VClL), x = -0.56, y = -0.40, z = 0.12, visual cortex lateral right (VClR) x= 0.56, y = -0.40, z = 0.12, and parietal midline (PM), x = 0.00, y = -0.50, z = 0.49, for the optic flow experiment, and visual cortex radial left (VCrL), x = -0.32, y = -0.55, z = 0.11, visual cortex radial right (VCrR), x = 0.32, y = -0.55, z = 0.11, and visual cortex ventral midline (VCvM), x = 0.00, y = -0.70, z = -0.08, for the looming experiment, as these are believed to be active in the visual processing of motion stimuli (Probst et al., 1993). Bone thickness was adjusted for infants at 3.0 mm and conductivity at 0.02σ.

The resulting time-frequency displays represented the change in amplitude over time in the regional sources. Since the focus was on induced oscillatory activity only, average evoked response signals were subtracted before computation of the TSE. For optic flow, separate TSEs for the different motion conditions, comparisons between each of the three motion conditions and the static condition, as well as between the combined motion condition and the static condition were performed. Bootstrapping statistics were used to investigate significant differences between the motion conditions and the static condition for each infant separately. For looming, separate TSEs for the different looming conditions based on selected looming peaks were performed. In addition, comparisons between the looming conditions, as well as a TSE of a combined motion condition were computed. Frequency cut-offs were set to 4-40 Hz, and frequency and time sampling were set at 1 Hz and 50 ms, respectively, for both experiments.

In analysis of induced activity in the optic flow data, BESA Statistics 1.0 was used to test for significant differences between the visual motion conditions and the static condition in

the TSE data for preterm and full-term infants at 4-5 and 12 months of age, separately. Statistical comparisons of the TSEs between the three visual motion conditions, as well as between the combined motion condition and the static condition were carried out. In analysis of induced activity in the looming data, the same software was used to test for significant differences between the three looming conditions in the TSE data for all groups, separately. Permutation testing in combination with data clustering was used to avoid the multiple comparisons problem. Cluster alpha, which determines the significance level for building clusters in time and/or frequency, was set at 0.005. The number of permutations was set at 512 (2^n, where n is the number of subjects), and the frequency cut-offs and epochs were kept the same as stated above. The comparisons allowed observation of significantly dominant oscillatory activities in the regional sources of interest for each infant.

3. Results

3.1 Optic flow

3.1.1 VEP responses

The four grand average channels of full-term infants at 4-5 months were POz, PO4, Oz and O2, and for the preterm infants at 4-5 months the four grand average channels were POz, PO4, Oz and O2. The four grand average channels of full-term infants at 12 months were PO4, PO8, O2 and Oz, and for the preterm infants at 12 months the grand average channels were PO3, POz, O1 and Oz. The selected channels that showed the highest mean N2 amplitudes in the forwards optic flow condition of the grand average VEPs are shown in Figure 4. Figure 5 shows the grand average VEPs for the three visual motion conditions for full-term infants at 4-5 months, preterm infants at 4-5 months, full-term infants at 12 months, and preterm infants at 12 months, respectively.

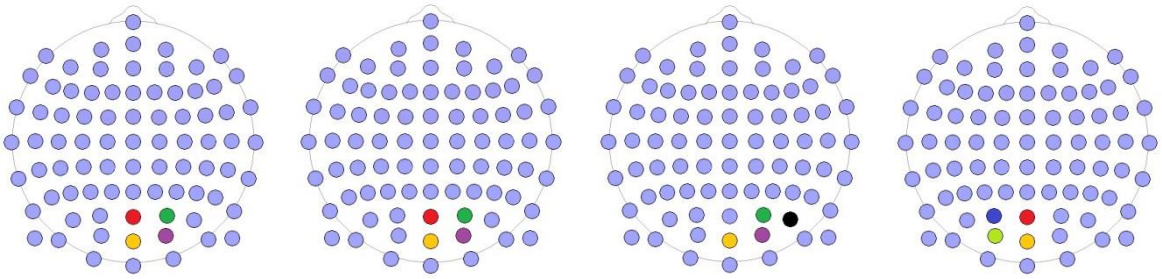

Figure 4. *Head drawings (nose up) showing the scalp localization of the 81 standard electrodes. From left to right: full-term infants 4-5 months, preterm infants 4-5 months, full-term infants 12 months, and preterm infants 12 months. The four electrodes of interest are indicated with color-filled circles: POz (**red**), PO4 (**green**), Oz (**orange**), O2 (**purple**), PO3 (**blue**), O1 (**light green**), and PO8 (**black**).*

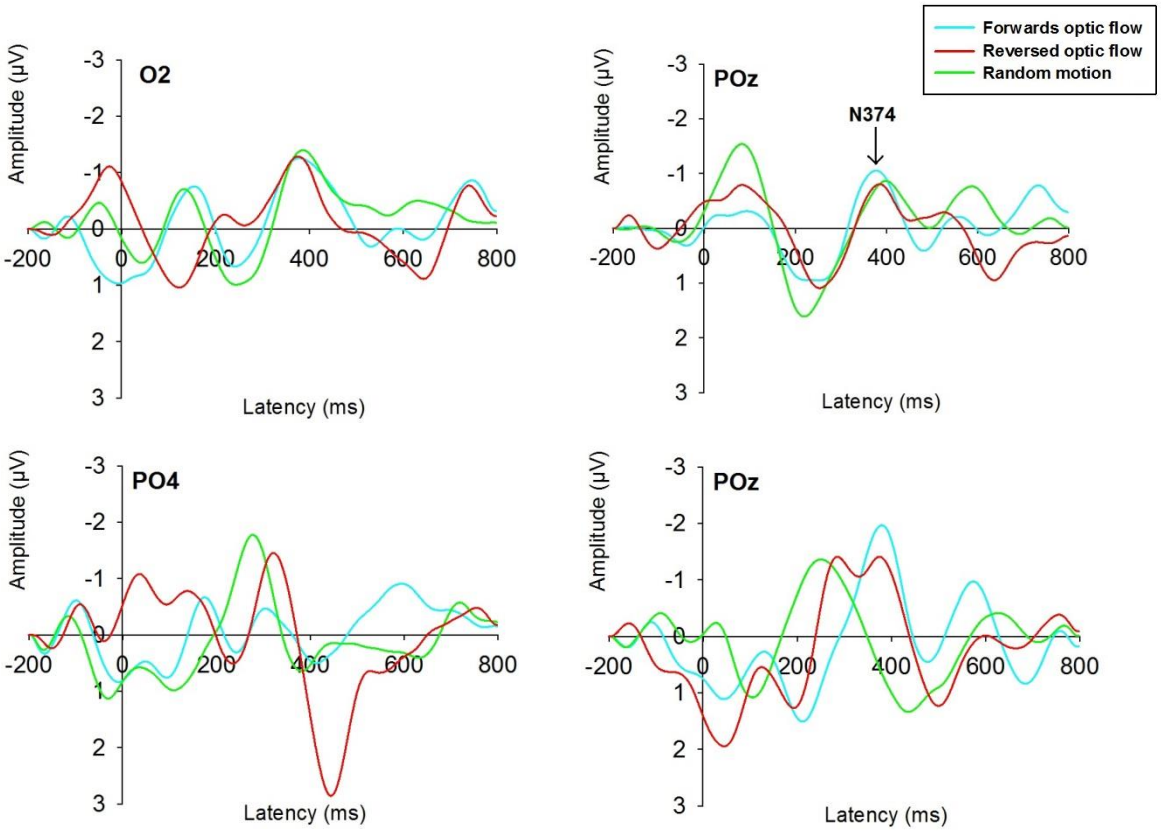

Figure 5. *Grand average motion VEPs in full-term infants at 4-5 months at the top left, preterm infants at 4-5 months at the top right, full-term infants at 12 months at the bottom left, and preterm infants at 12 months at the bottom right for forwards optic flow (**blue**), reversed optic flow (**red**), and random motion (**green**). The N2 peak for forwards optic flow is marked with actual latency at the POz electrode for preterm infants at 4-5 months. The epoch is from -200 ms to 800 ms.*

3.1.2 Latency analysis of VEPs

The mean N2 latency for full-term infants at 4-5 months of age for the three motion conditions forwards optic flow, reversed optic flow and random motion was 380 ms (SD = 48 ms), 433 ms (SD = 64 ms), and 459 ms (SD = 57 ms), respectively. For the preterm infants at 4-5 months, the mean N2 latency for the three motion conditions was 310 ms (SD = 58 ms), 337 ms (SD = 54 ms), and 362 ms (SD = 60 ms), respectively. The mean N2 latency for the three motion conditions for full-term infants at 12 months was 265 ms (SD = 46 ms), 315 ms (SD = 32 ms), and 411 ms (SD = 55 ms), respectively. For the preterm infants at 12 months, the mean N2 latency for the three motion conditions was 380 ms (SD = 47 ms), 385 ms (SD = 62 ms), and 386 ms (SD = 64 ms), respectively.

Latencies of the VEPs were analyzed using repeated measures ANOVAs in a 2 (group: full-term and preterm) x 2 (age: 4-5 and 12 months) x 3 (visual motion condition) factor

design. Adjustment for multiple comparisons was made by Bonferroni correction. The electrode that showed the largest N2 amplitude in the forward optic flow condition was used in the ANOVA. The electrode used varied across participants, but was always one of the four posterior electrodes selected from the grand averages of the separate groups, and was the same for the three motion conditions in each infant.

A significant three-way interaction of condition, age and group was found, F (2, 32) = 4.29, $P < 0.05$, indicating that significant latency differences between the motion conditions were found only for the full-term infants at 12 months. The results indicate that for full-term infants at 12 months, latencies for forwards optic flow were shorter than for reversed optic flow, and that latencies for reversed optic flow were shorter than for random motion (see Figure 6). The preterm infants, on the other hand, did not differentiate between the three visual motion conditions, neither at 4-5 nor at 12 months. In addition, the ANOVA revealed a significant two-way interaction of age and group, F (1, 16) = 35.62, $P < 0.001$, indicating that at 4-5 months of age, the preterm infants had significantly shorter N2 latencies than the full-term infants irrespective of visual motion condition, but that at 12 months, the full-term infants had significantly shorter N2 latencies than the preterm infants. In addition, the two-way interaction of age and group indicates that only the full-term infants significantly reduced their N2 latencies with age, especially for the two optic flow conditions.

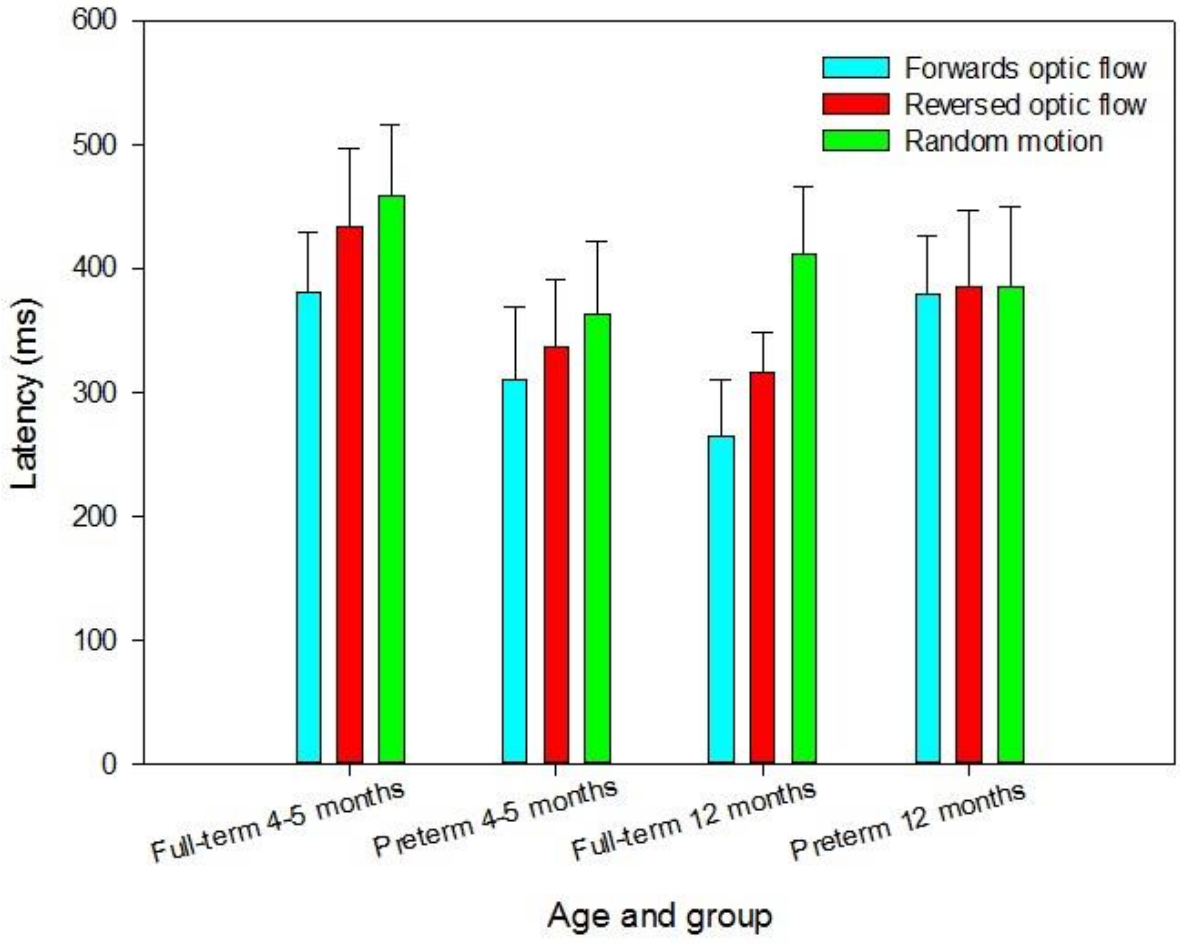

Figure 6. *Means (and SDs) of peak latencies for the three motion conditions in preterm and full-term infants at 4-5 and 12 months of age. Mean latency decrease from random motion, to reversed optic flow, to forwards optic flow was significant only for full-term infants at 12 months. The latencies decreased significantly with age for the full-term infants, but not for the preterm infants. In addition, preterm infants at 4-5 months of age had significantly shorter latencies in all three motion conditions than their full-term peers.*

3.1.3 Individual analysis of optic flow VEPs

The latency data from the full-term and preterm infants at 12 months of age were further explored in order to investigate whether some preterm infants were especially delayed in their responses to optic flow, leading to difficulties with perceiving visual motion. An outlier value was defined as a value larger or smaller than mean $\pm$ SD*2.5, as formulated by Field (2009). Mean $\pm$ SD*2.5 was calculated for the three visual motion conditions for the 12-month-old full-term infants, and the 12-month-old preterm infants who showed latencies above these criterion values were marked (see Table 1). Three preterm infants, AT, DA and MS, were pointed out based on the criterion. These preterm infants showed extremely long latencies for both forwards and reversed optic flow. In addition, two infants, SE and WM, showed longer

latencies for forwards optic flow only. However, none of these five preterm infants showed delayed motor development at the time of the second testing, although SE and WM were both bottom shufflers.

Full-term	**Forwards**	**Reversed**	**Random**	**Preterm**	**Forwards**	**Reversed**	**Random**
AK	348	372	430	AT	462	408	348
BK	186	300	370	DK	336	364	316
BE	296	332	436	DA	390	506	460
GE	294	336	456	EL	294	272	304
HD	262	284	454	FP	366	390	342
JY	256	332	396	MS	392	408	484
LS	228	304	328	SE	398	350	374
SA	250	314	342	TA	370	392	412
SN	262	262	488	WM	408	374	430
Mean	265	315	411		380	385	386
SD	46	32	55		47	62	64
Mean+SD*2.5	**379**	**396**	**549**				

Table 1. *Average VEP latencies (ms) for the three visual motion conditions for 12-month-old full-term and preterm infants. The marked numbers indicate the preterm infants who showed latency values greater than mean+ SD*2.5 of the VEP latency values of the full-term group. Preterm infants AT, DA and MS stood out with their long latencies for both optic flow conditions. In addition, preterm infants SE and WM showed outlier values for forwards optic flow only.*

3.1.4 TSE analysis

For full-term infants at 4-5 months, the TSE of the motion condition was seen as desynchronized activity, which occurred in the same frequency band as the synchronized activity observed in the TSE of the static dot pattern (see Figure 7a and 7b). This is especially evident in the TSE of the comparison between the motion condition and the static dot pattern (see Figure 7c), where the largest differences in activity can be observed in the theta-band range. Average frequency of the maximum induced ERD for the three visual sources of interest was 5.8 Hz (SD = 1.8), with mean latency of 699 ms (SD = 126). Figure 7d displays the results of the bootstrapping procedure for full-term infant participant JY when the TSE of the motion condition was compared to the TSE of the static dot pattern. The Figure shows that the theta-band induced activity in regional sources VClL, PM and VClR was significantly different in the motion condition compared to the static dot pattern.

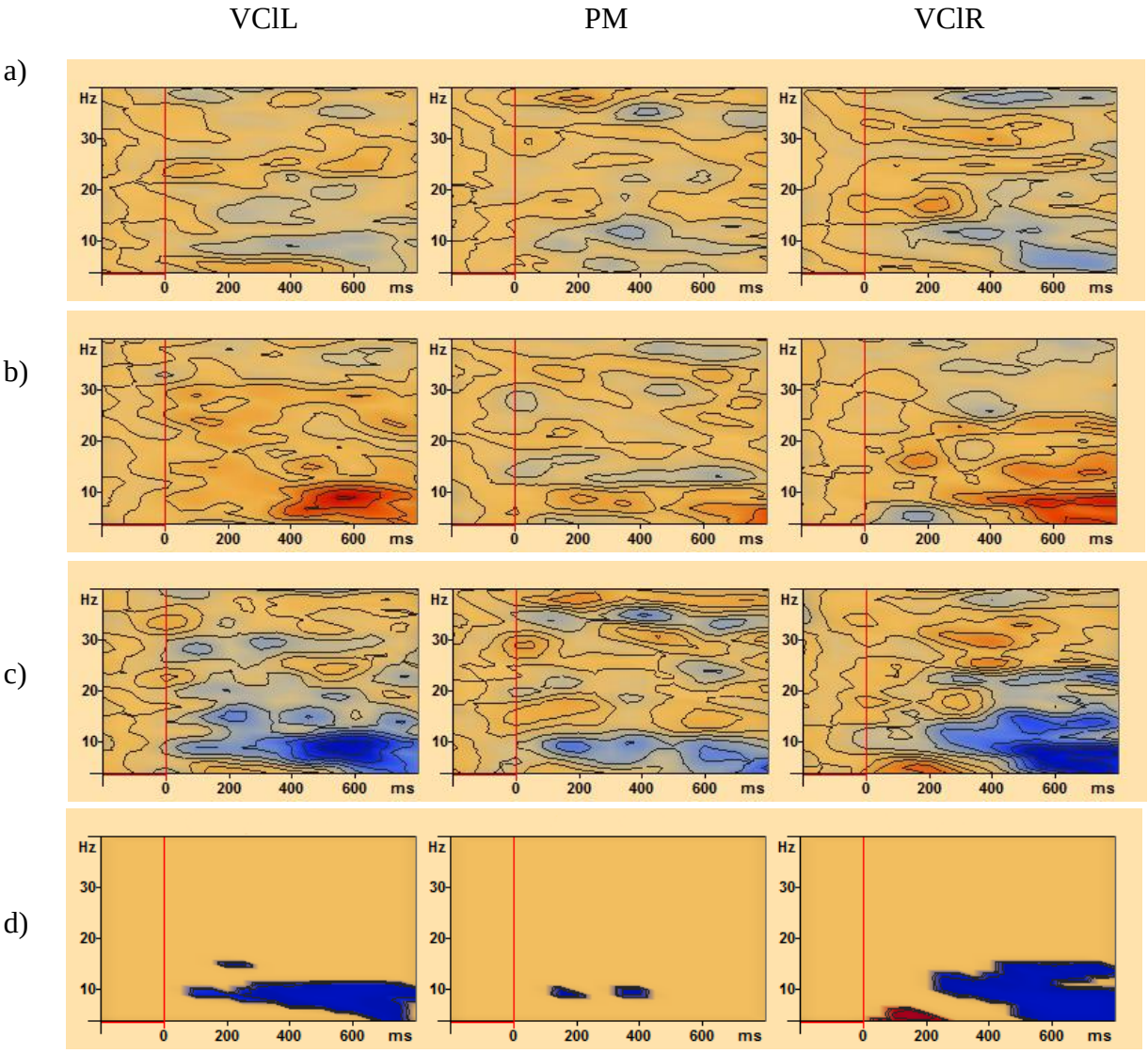

Figure 7 a), b) *TSE maps of motion a) and static b) with epoch length of 800 ms for full-term infant JY at 4 months. VClL, PM and VClR represent the visual areas of interest. Stimulus onset at 0 ms is marked with a red vertical line. Blue areas represent desynchronized activity, while red areas represent synchronized activity. Desynchronization in the theta-band range can be observed in the TSE of the motion condition a), while synchronization in the theta-band range can be observed in the TSE of the static dot pattern b).*
c) *TSE map of the comparison between the motion condition and the static dot pattern for full-term infant JY. The strong blue color in the theta-band frequency after 400 ms represents the area with the largest change in activity. Note that the same areas showed up as significant in the results of the bootstrapping procedure d).*
d) *Results of bootstrapping procedure showing TSE probability maps for full-term infant JY comparing the motion condition with the static dot pattern. The blue areas indicate significant decrease in TSE, while red areas indicate significant increase in TSE. Significant induced desynchronization (decrease in TSE) can be observed at theta-band frequencies.*

Similar results were obtained for preterm infants at 4-5 months of age. The TSE of the motion condition showed desynchronized activity, which occurred in the same frequency band as the synchronized activity observed in the TSE of the static dot pattern (see Figure 8a and b). Average frequency of the maximum induced ERD for the three visual sources of interest was 6.2 Hz (SD = 1.7), with mean latency of 748 ms (SD = 104). Figure 8c displays the TSE of the comparison between the motion and the static condition. The results of the bootstrapping procedure for preterm infant MS when the TSE of the motion condition was compared to the TSE of the static dot pattern shows that induced desynchronized activity in the theta band was significantly different in the motion condition compared to the static dot pattern (Figure 8d).

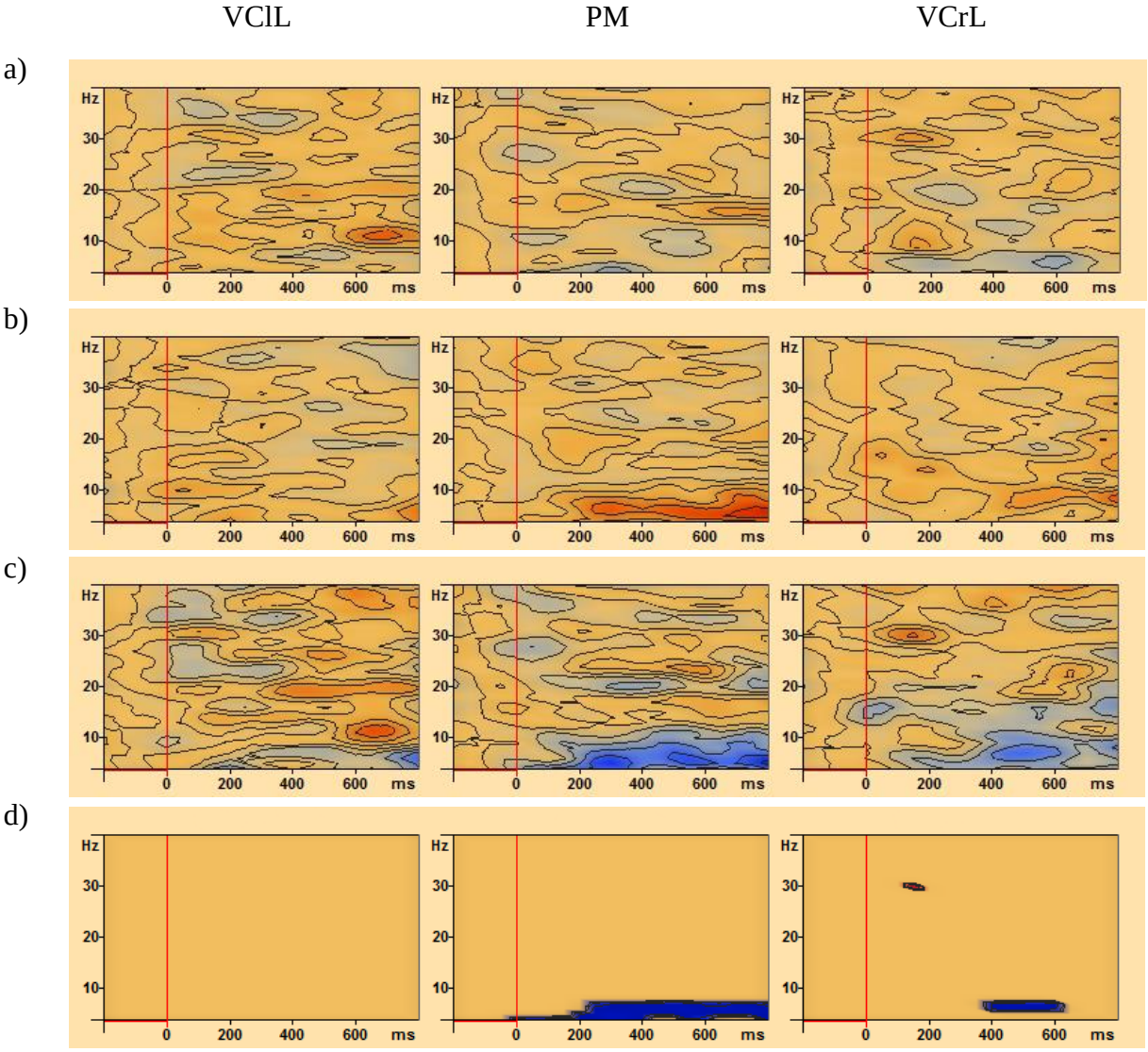

Figure 8 a), b) *TSE maps of motion a) and static b) with epoch length of 800 ms for preterm infant MS at 5 months. VClL, PM and VClR represent the visual areas of interest. Stimulus onset at 0 ms is marked with a red vertical line. Blue areas represent desynchronized activity, while red areas represent synchronized activity. Desynchronization in the theta-band range can be observed in the TSE of the motion condition a), while synchronization in the theta-band range can be observed in the TSE of the static dot pattern b).*
c) *TSE map of the comparison between the motion condition and the static dot pattern for preterm infant MS. The strong blue color in the theta-band frequency after 400 ms represents the area with the largest change in activity. Note that the same areas showed up as significant in the results of the bootstrapping procedure d).*
d) *Results of bootstrapping procedure showing TSE probability maps for preterm infant MS comparing the motion condition with the static dot pattern. The blue areas indicate significant decrease in TSE, while red areas indicate significant increase in TSE. Significant induced desynchronization (decrease in TSE) can be observed at theta-band frequencies.*

For 12-month-old full-term infants, the TSE of the motion condition was seen as desynchronized activity in the theta frequency range. In addition, synchronized activity within the late alpha and early beta ranges was observed, peaking at approximately 334 ms after stimulus start. The synchronized activity occurred in the same frequency band as the desynchronized activity observed in the TSE of the static dot pattern (see Figure 9a and 9b). This can be observed in the TSE map of the comparison between the motion condition and the static dot pattern (see Figure 9c). Average frequency of the maximum induced ERS for the three visual sources of interest was 18.4 Hz (SD = 8.0), with mean latency of 334 ms (SD = 171). Figure 9d displays the results of the bootstrapping procedure for full-term infant participant JY when the TSE of the motion condition was compared to the TSE of the static dot pattern. The Figure shows that induced synchronized activity in the alpha band and desynchronized activity in the theta band was significantly different in the motion condition compared to the static dot pattern.

For preterm infants at 12 months of age, the TSE of the motion condition showed desynchronized activity in the theta range, similar to what was observed when the same infants were 4-5 months of age. Average frequency of the maximum induced ERD for the three visual sources of interest was 8.8 Hz (SD = 4.2), with mean latency of 665 ms (SD = 171). In addition, some synchronized activity in the late alpha and early beta band, around 18.7 Hz, was observed approximately 391 ms after stimulus start, but this was less prominent than in the full-term infants, and some preterm infants' TSEs did not show similar activity at all. Figure 10a displays the TSEs of 12-month-old preterm infant SE, where desynchronized activity in the motion condition occurred in the same frequency band as the synchronized activity observed in the TSE of the static dot pattern (see Figure 10b). Figure 10c shows the TSE of the comparison between the motion condition and the static dot pattern. Little to no synchronized activity within the late alpha and early beta range around 300-400 ms can be observed. The results of the bootstrapping procedure (see Figure 10d) confirm that there is no significant difference in synchronized activity when the motion condition is compared to the static dot pattern. Similar results were observed in preterm infants DA and EL (see Appendix A).

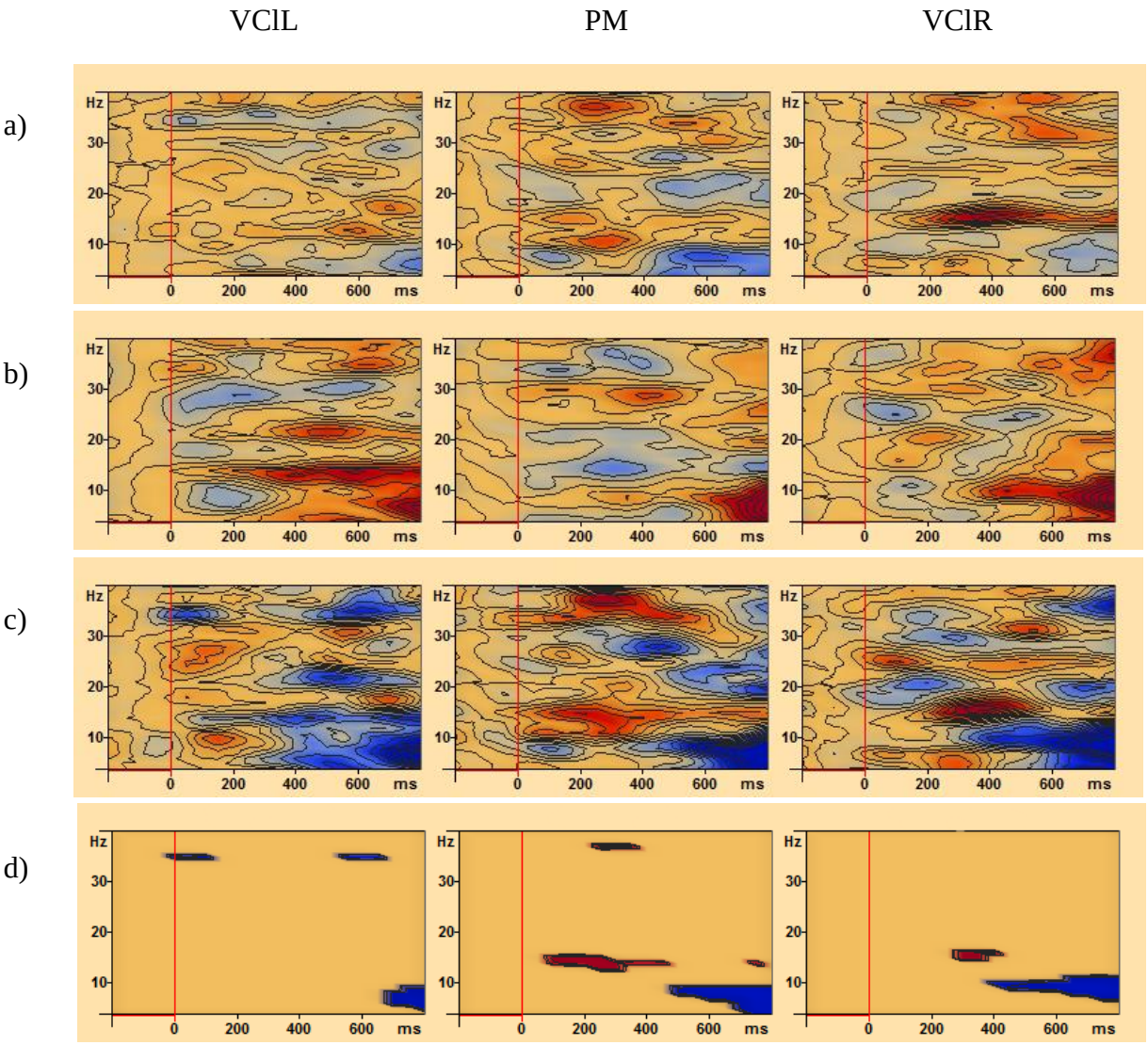

Figure 9 a), b) *TSE maps of motion a) and static b) with epoch length of 800 ms for full-term infant JY at 12 months. VClL, PM and VClR represent the visual areas of interest. Stimulus onset at 0 ms is marked with a red vertical line. Blue areas represent desynchronized activity, while red areas represent synchronized activity. In addition to desynchronization in the theta-band range, as observed at 4-5 months of age, synchronization in the alpha-band frequency can be observed in the TSE of the motion condition a), while desynchronization in the alpha-band range can be observed in the TSE of the static dot pattern b).*

c) *TSE map of the comparison between the motion condition and the static dot pattern for full-term infant JY at 12 months. The strong blue color in the theta-band frequency after 400 ms, and the strong red color in the alpha-band frequency around 200-300 ms, represents the area with the largest change in activity. Note that the same areas showed up as significant in the results of the bootstrapping procedure d).*

d) *Results of bootstrapping procedure showing TSE probability maps for full-term infant JY at 12 months comparing the motion condition with the static dot pattern. The blue areas indicate significant decrease in TSE, while red areas indicate significant increase in TSE. Significant induced desynchronization (decrease in TSE) can be observed at theta-band frequencies, while significant induced synchronization (increase in TSE) can be observed at alpha-band frequencies.*

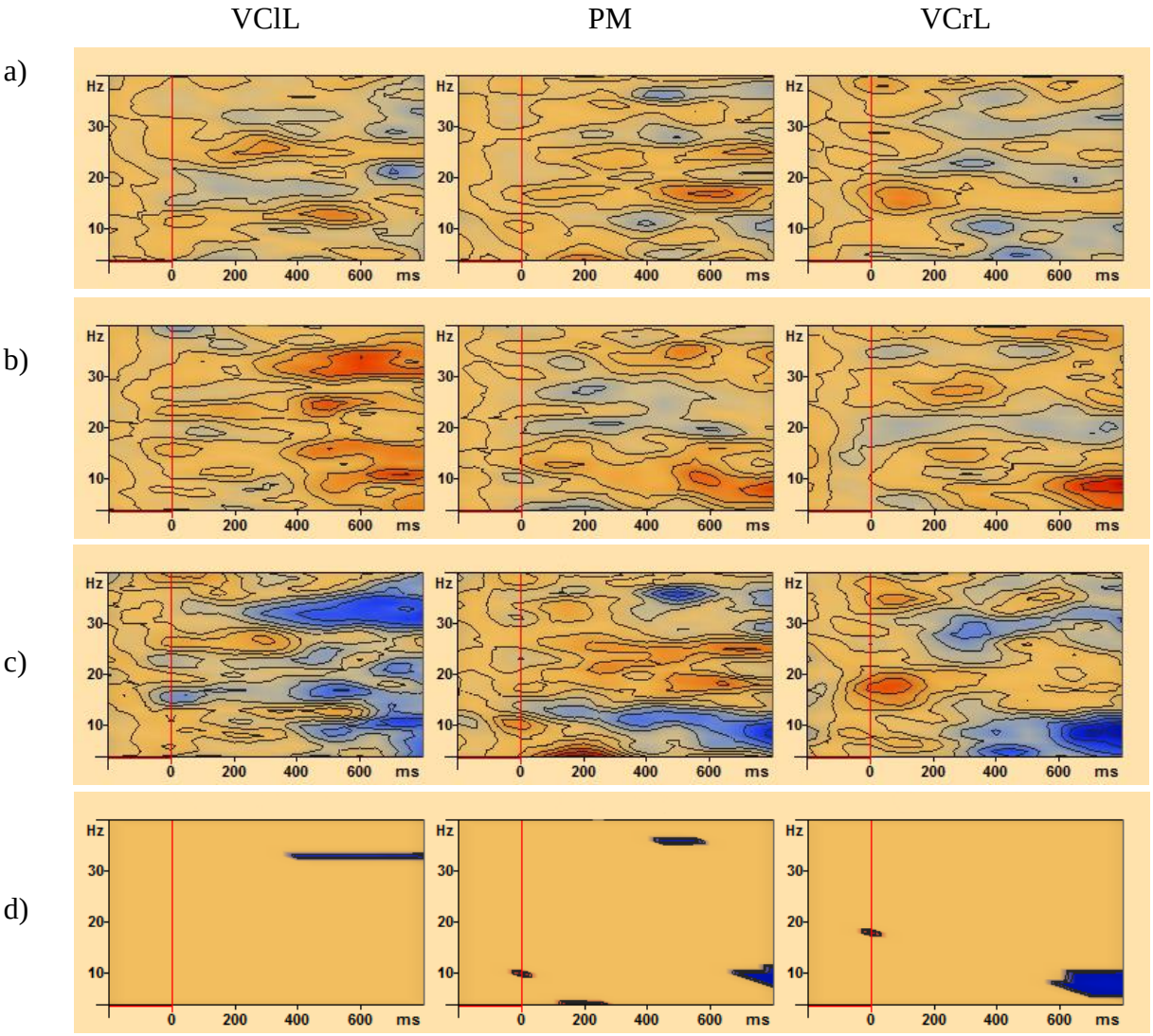

Figure 10 a), b) *TSE maps of motion a) and static b) with epoch length of 800 ms for preterm infant SE at 12 months. VClL, PM and VClR represent the visual areas of interest. Stimulus onset at 0 ms is marked with a red vertical line. Blue areas represent desynchronized activity, while red areas represent synchronized activity. Desynchronization in the theta-band range can be observed in the TSE of the motion condition a), while synchronization in the theta-band range can be observed in the TSE of the static dot pattern b).*

c) *TSE map of the comparison between the motion condition and the static dot pattern for preterm infant SE at 12 months. The strong blue color in the theta-band frequency after 400 ms represents the area with the largest change in activity. Note that the same areas showed up as significant in the results of the bootstrapping procedure d).*

d) *Results of bootstrapping procedure showing TSE probability maps for preterm infant SE at 12 months comparing the motion condition with the static dot pattern. The blue areas indicate significant decrease in TSE, while red areas indicate significant increase in TSE. Significant induced desynchronization (decrease in TSE) can be observed at theta-band frequencies in visual areas PM and VClR.*

Figure 11 displays the results of the permutation tests for regional sources VClL, PM (all groups apart from full-terms at 4-5 months) and VClR for the average of 4-5-month-old full-terms (Figure 11a) and preterms (Figure 11b), and 12-month-old full-terms (Figure 11c) and preterms (Figure 11d) when the TSE of the motion condition was compared to the TSE of the static dot pattern. The results of the permutation test for the comparison of the motion and static condition showed significant negative clusters in the regional sources of interest indicating that the motion condition had significantly lower amplitude values in the theta-band range than the static condition. The permutation tests did not show any significant positive clusters in higher frequencies in any of the four groups, likely due to individual frequency and latency differences. No significant differences were found between the three separate motion conditions, forwards optic flow, reversed optic flow, and random motion, when they were each compared with the other.

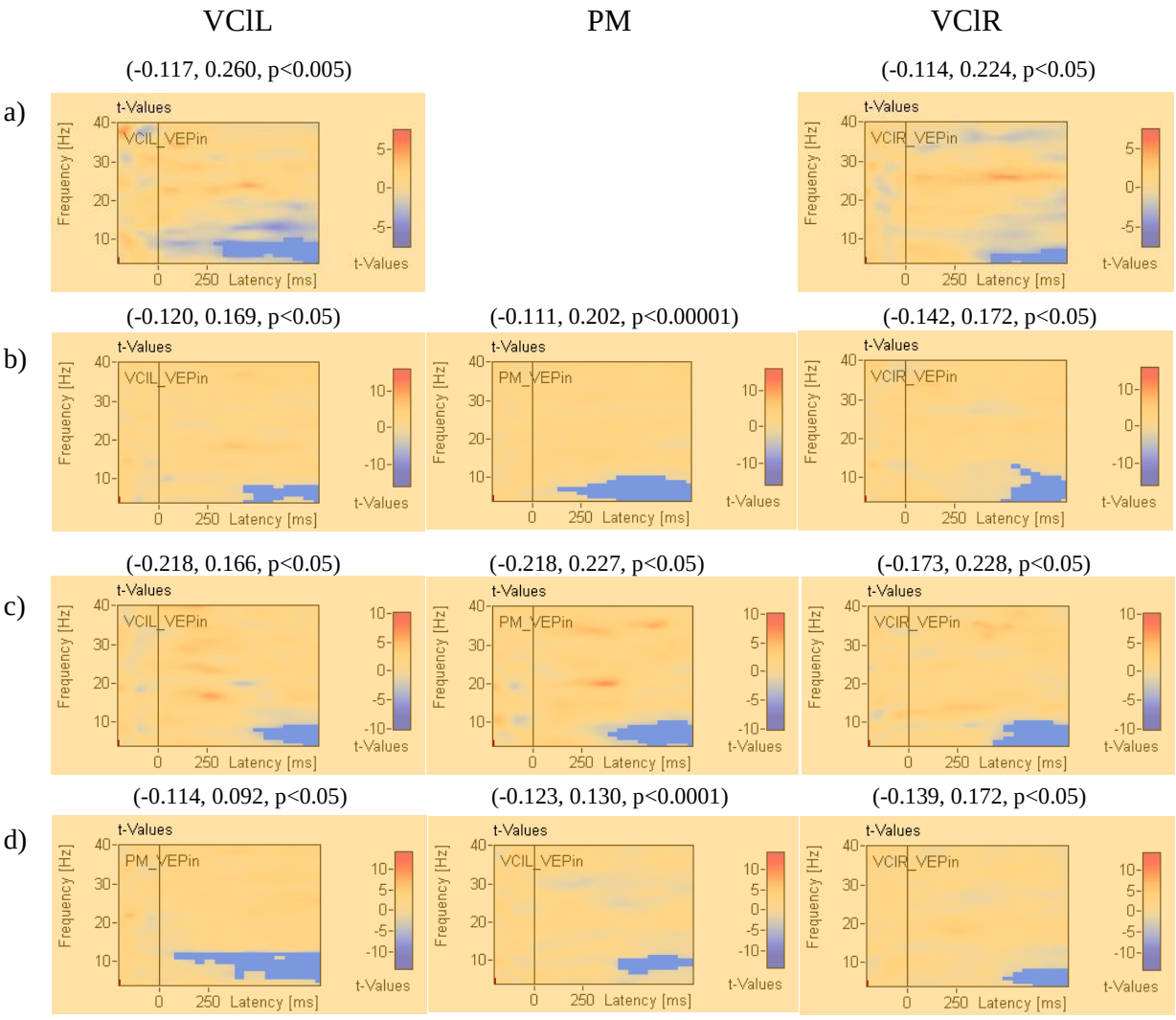

Figure 11. *Average visualization of significant data clusters in the regional sources of interest when the motion condition was compared with the static condition for full-term infants at 4-5 months a), preterm infants at 4-5 months b), full-term infants at 12 months c), and preterm infants at 12 months d). Blue indicates negative clusters (i.e. the motion condition had smaller t-values than the static condition); while red indicates positive clusters (i.e. the motion condition had larger t-values then the static condition). The black vertical line indicates stimulus onset. Each visual area is dominated by activity in the theta-band range. Cluster means for the motion condition and the static condition, as well as the probability level are presented in parentheses.*

3.2 Looming

3.2.1 VEP responses

Looming-related VEP responses were observed in the occipital and parietal areas of the cortex prior to the time when the loom would have made contact with the infant. Data were recorded from the Oz and Pz channels. Due to a lack of data in Pz, only data collected from the Oz channel were used for further analysis. In total, infants provided 459 trials in which the looming stimuli provided a looming-related peak. Each infant provided an average of 13 (SD = 2) trials where prominent looming-related peaks were observed during each testing session. The looming-related peaks were evenly distributed among the three loom speeds.

At 4-5 months, full-term infants showed their looming-related VEPs on average -1.15 s (SD = 0.28), and at 12 months -0.48 s (SD = 0.11) prior to the visual collision. Preterm infants showed their looming-related VEPs on average -1.07 s (SD = 0.24) at 4-5 months of age, and at 12 months -1.00 s (SD = 0.21) prior to the virtual collision.

Repeated measures ANOVA was used to test for differences in averaged looming-related peak activation among full-term and preterm infants at 4-5 and 12 months of age. Bonferroni correction was used for adjustment for multiple comparisons. A 2 (group) x 2 (age) x 3 (looming condition) repeated measures ANOVA revealed a three-way interaction effect of age, group, and looming condition, $F(2, 32) = 4.68$, $P < 0.05$. This result indicates that the looming-related VEPs occurred closer to the time of the virtual collision with increasing age, but that only the 12-month-old full-term infants showed their averaged looming-related VEPs at a fixed time-to-collision of approximately -0.48 s, irrespective of loom speed (see Figure 12). A two-way interaction effect of age and group, $F(1, 16) = 89.15$, $P < 0.005$ indicates that only the full-term infants significantly reduced their time-to-collision with age (see Figure 12).

In addition, the results revealed a main effect of age, $F(1, 16) = 142.88$, $P < 0.005$. However, this effect is not real due to the fact that only the full-term infants significantly decreased their time-to-collision with age (see Figure 12).

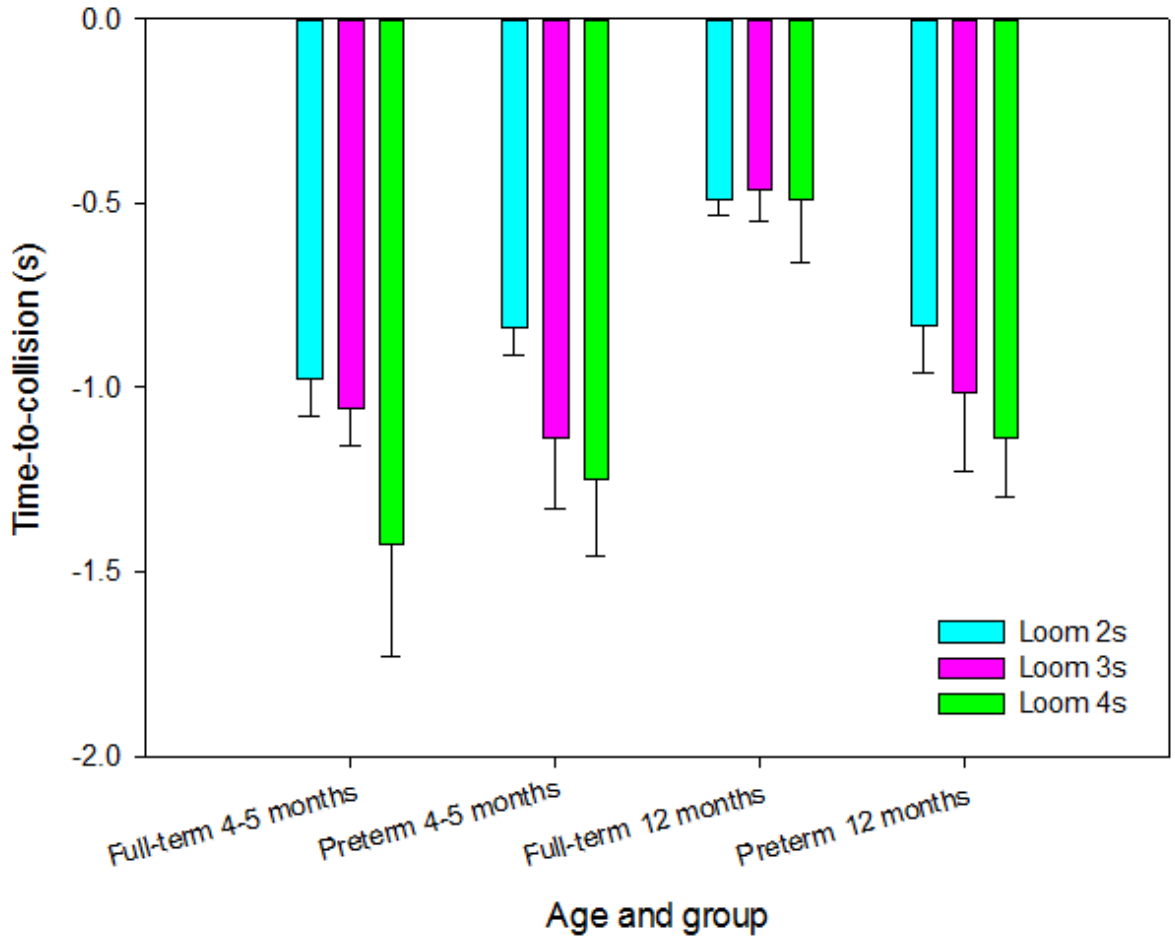

Figure 12. *Averaged looming-related VEP peak responses (and SDs) for the three looming conditions in full-term and preterm infants at 4-5 and 12 months of age. With age, both full-term and preterm infants responded at smaller values of time-to-collision, although the decrease was significant for the full-term infants only. At 12 months, full-term infants responded significantly closer to the time of collision than preterm infants. In addition, only full-term infants at the age of 12 months showed their averaged looming-related responses at a fixed time-to-collision, at approximately -0.48s.*

3.2.2 Individual analysis of looming VEP responses

The averaged looming-related VEP responses from full-term and preterm infants at 12 months of age were further explored in order to investigate whether some preterm infants were using a less efficient timing strategy when responding to the different looming speeds. An outlier value was defined in the same way as for the individual optic flow VEP analysis. Mean ± SD*2.5 was calculated for the standard deviation between the three looming conditions for the 12-month-old full-term infants, and the 12-month-old preterm infants who showed standard deviations above these criterion values were marked (see Table 1). A large standard deviation indicates that the averaged looming-related VEP responses are distant from the

mean (Field, 2009), and thus indicate that the infant was not using a timing strategy based on time, which would be indicated by a low standard deviation (i.e. the infant responds at a fixed time-to-contact, irrespective of loom speed). Three preterm infants, AT, EL and SE, were pointed out based on the criterion as they showed unusually high standard deviations. None of these three preterm infants showed delayed motor development at the time of the second testing, although SE was a bottom shuffler.

Full-term	**2s**	**3s**	**4s**	**SD**	**Preterm**	**2s**	**3s**	**4s**	**SD**
AK	-0.470	-0.516	-0.663	0.101	AT	-0.871	-1.021	-1.377	0.260
BK	-0.483	-0.563	-0.576	0.050	DK	-1.043	-0.957	-1.001	0.043
BE	-0.551	-0.454	-0.108	0.233	DA	-0.976	-1.121	-1.322	0.174
GE	-0.499	-0.572	-0.586	0.047	EL	-0.729	-1.491	-0.956	0.391
HD	-0.443	-0.424	-0.504	0.042	FP	-0.732	-0.861	-1.109	0.192
JY	-0.529	-0.345	-0.616	0.138	MS	-0.809	-0.913	-1.144	0.171
LS	-0.448	-0.448	-0.359	0.051	SE	-0.714	-1.093	-1.306	0.300
SA	-0.459	-0.349	-0.497	0.077	TA	-0.690	-0.717	-1.034	0.191
SN	-0.548	-0.514	-0.517	0.019	WM	-0.936	-0.948	-0.994	0.031
Mean				0.084					0.195
SD				0.066					0.115
Mean + SD*2.5				**0.250**					

Table 2. *Average looming-related VEP responses (ms) and standard deviations for the three looming conditions for all 12-month-old full-term and preterm infants. The marked numbers indicate the preterm infants who showed standard deviations greater than mean+ SD*2.5 of the standard deviations of the full-term group. Preterm infants AT, EL and SE stood out with their high standard deviation indicating that these infants had unusually large differences in response time to the three looming conditions which could be indicative of these infants gearing their looming-related VEP responses not to time-to-collision, but to the visual angle of the approaching virtual object.*

3.2.3 TSE analysis

For full-term infants at 4-5 months, the TSE of the combined looming condition was seen as synchronized activity in the theta frequency range in one or more visual areas, with an average frequency of maximum induced synchronization of 5.5 Hz (SD = 1.9) peaking at approximately 194 ms (SD = 74) after the time at which the looming-related VEP peak occurred. In addition, early alpha-band desynchronization was observed, with an average frequency of maximum induced desynchronization of 9.6 Hz (SD = 3.7), peaking at approximately 183 ms (SD = 83) after the time at which the looming-related VEP peak was observed (Figure 13, also see Appendix B). There were no significant differences between the three separate looming conditions when they were compared with each other.

VCrL VCvM VCrR

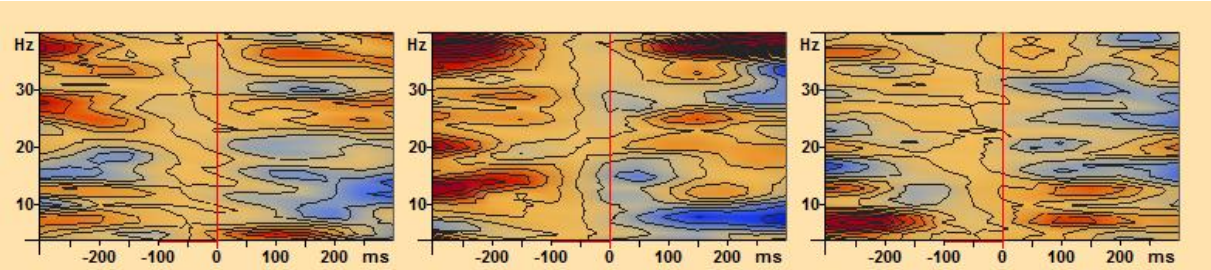

Figure 13. *TSE maps of the combined looming condition with epoch length of -300 to 300 ms for full-term infant GE at 5 months. VCrL, VCvM and VCrR represent the visual areas of interest. A red vertical line indicates the top of the observed looming-related VEP peak. Blue areas represent desynchronized activity, while red areas represent synchronized activity. Synchronized activity can be observed in the theta frequency range in visual sources VCrL and VCrR. In addition, desynchronized activity in the early alpha frequency range can be observed in visual sources VCrL and VCvM. Some synchronization in the late alpha frequency range can be observed.*

Similar results were observed in the TSEs for preterm infants at 4-5 months. The TSE of the combined looming condition was seen as synchronized activity in the theta frequency range in one or more visual areas in all but one preterm infant, with an average frequency of maximum induced synchronization of 5.7 Hz (SD = 1.5) peaking at approximately 212 ms (SD = 73) after the time at which the looming-related VEP peak was observed. In addition, early alpha-band desynchronization was observed in two or more visual areas, with an average frequency of maximum induced desynchronization of 10.4 Hz (SD = 3.9), peaking at approximately 215 ms (SD = 71) after the time at which the looming-related VEP peak was observed (Figure 14, also see Appendix B). Again, there were no significant differences between the three separate looming conditions when they were compared with each other.

VCrL VCvM VCrR

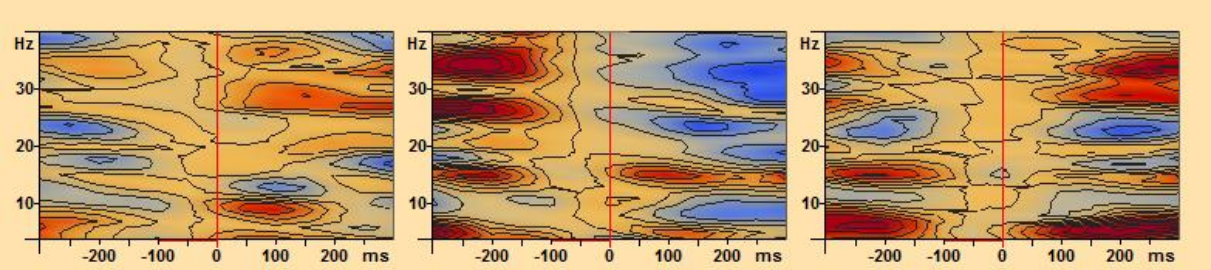

Figure 14. *TSE maps of the combined looming condition with epoch length of -300 to 300 ms for preterm infant SE at 4 months. VCrL, VCvM and VCrR represent the visual areas of interest. A red vertical line indicates the top of the observed looming-related VEP peak. Blue areas represent desynchronized activity, while red areas represent synchronized activity. Synchronized activity can be observed in the theta frequency range in all visual sources of interest. In addition, desynchronized activity in the early alpha frequency range can be observed in all visual sources of interest. Some synchronization in the late alpha frequency can be observed in visual sources VCvM and VCrR.*

For 12-month-old full-term infants, the TSE of the combined looming condition was seen as synchronized activity in the theta frequency range in two or more visual areas of interest in all but one full-term infant, with an average frequency of maximum induced synchronization of 5.4 Hz (SD = 2.2), peaking at approximately 243 ms (SD = 63) after the time at which the looming-related VEP peak was observed. As seen in the same group at 4-5 months, alpha band desynchronization was observed with an average frequency of maximum induced desynchronization of 12.0 Hz (SD = 3.6), peaking at approximately 219 ms (SD = 60) after the time at which the looming-related VEP peak was observed. In addition, high synchronized activity was observed in one or more visual sources of interest in the late alpha and early beta frequency ranges with an average frequency of maximum induced synchronization of 18.3 Hz (SD = 5.4), peaking at approximately 219 ms (SD = 72) after the time at which the looming-related VEP peak was observed (Figure 15, also see Appendix B). There were no significant differences between the three separate looming conditions when they were each compared with the other.

VCrL VCvM VClL

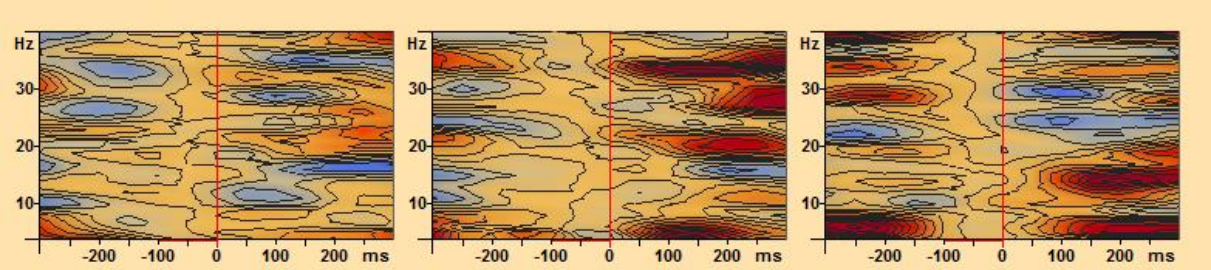

Figure 15. *TSE maps of the combined looming condition with epoch length of -300 to 300 ms for full-term infant GE at 12 months. VCrL, VCvM and VCrR represent the visual areas of interest. A red vertical line indicates the top of the observed looming-related VEP peak. Blue areas represent desynchronized activity, while red areas represent synchronized activity. In addition to synchronized activity in the theta frequency range and desynchronized activity in the alpha frequency range, high synchronized activity can be observed in the late alpha and early beta frequency range.*

For preterm infants at 12 months of age, the TSE of the combined looming condition showed results similar to what was seen in the same group at 4-5 months. Synchronized activity in the theta frequency range was observed in two or more visual sources of interest, with an average frequency of maximum induced synchronization of 5.7 Hz (SD = 1.8), peaking at approximately 220 ms (SD = 68) after the time at which the looming-related VEP peak was observed. Desynchronized activity was observed in two or more visual sources of interest, with an average frequency of maximum induced synchronization of 10.8 Hz (SD = 3.4), peaking at approximately 242 ms (SD = 56) after the time at which the looming-related VEP peak was observed. In addition, some synchronized activity was observed in one or more visual sources of interest in the late alpha and early beta frequency ranges with an average frequency of maximum induced synchronization of 19.2 Hz (SD = 4.2), peaking at approximately 203 ms (SD = 78) after the time at which the looming-related VEP peak was observed (see Appendix B). However, not all preterm infants showed synchronization at higher frequencies. Figure 16 displays the TSE maps for preterm infants AT (Figure 16a) and DA (Figure 16b), where little to no synchronization can be observed in the late alpha and early beta frequencies. Again, there were no significant differences between the three separate looming conditions when they were each compared with the other.

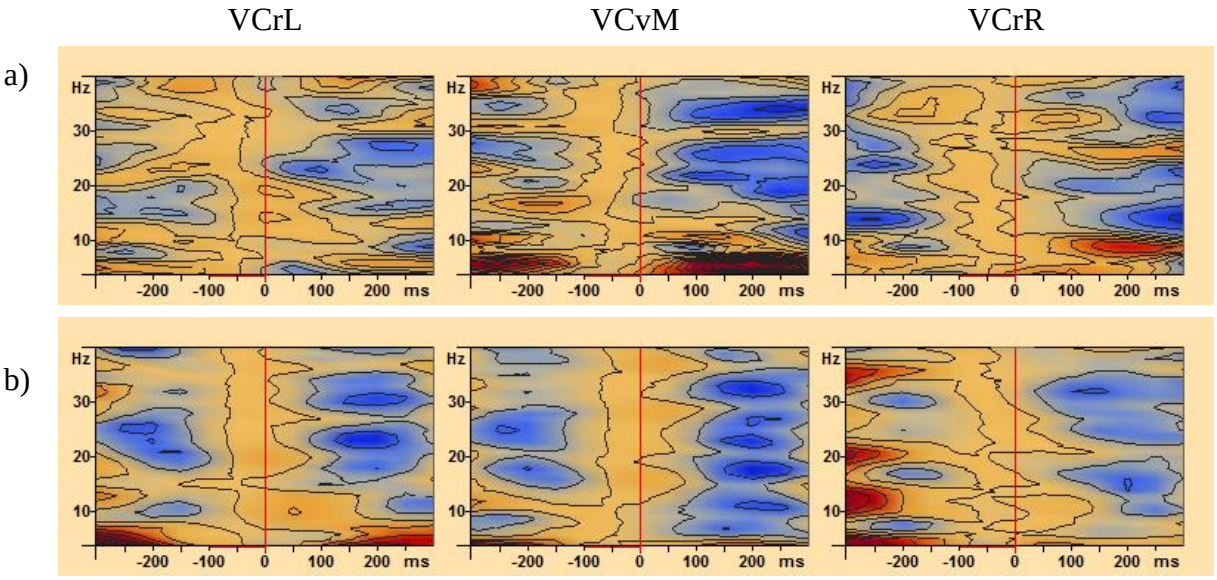

Figure 16. *TSE maps of the combined looming condition with epoch length of -300to 300 ms for preterm infant AT a), and preterm infant DA b), at 12 months. VCrL, VCvM and VCrR represent the visual areas of interest. A red vertical line indicates the top of the observed looming-related VEP peak. Blue areas represent desynchronized activity, while red areas represent synchronized activity. Synchronized activity can be observed in visual sources a) VCvM and VCrR and b) VCrL and VCvM. In addition, desynchronized activity in the early alpha frequency range can be observed in all visual sources.*

4. Discussion

In the present study, high-density EEG was used to longitudinally study brain electrical activity as a function of perception of visual motion stimuli in full-term and preterm infants at 4-5 and 12 months of age. The infants were presented with two visual motion paradigms: optic flow and looming. The optic flow experiment consisted of three visual motion stimuli simulating forwards and reversed optic flow and random visual motion, in addition to a static dot pattern used as a control condition. The looming experiment simulated a virtual object on a collision course approaching the infants at three different speeds. VEP and TSE analyses were used to investigate differences in evoked and induced brain electrical activity between the groups, so as to see whether the preterm infants showed an abnormal development of visual motion perception compared to their full-term peers, indicating a possible dorsal stream vulnerability.

The VEP analysis of optic flow data revealed that during the course of development from 4-5 to 12 months of age, only full-term infants significantly reduced their VEP latencies, especially for the two optic flow conditions. This could indicate that with increasing age, full-term infants become more sensitive to structured optic flow, supporting earlier findings of a longitudinal study investigating the development of visual motion processing in full-term infants at 3-4 and 11-12 months of age (Agyei et al., 2014). The VEP analysis of looming data revealed a similar result, where only the full-term infants significantly reduced the time-to-collision of their looming-related VEP responses from 4-5 to 12 months of age.

Long response times were observed in both full-terms and preterms at 4-5 months of age, and could be a result of a larger amount of coherently activated neurons, likely indicating a lack of specialized neuronal networks in the infant brain (Johnson, 2000; Dubois et al., 2006). The significant decrease in the latency of the N2 component of the VEP waveforms which is observed in the full-term infants' optic flow data, and the decrease in time-to-collision of the looming-related VEP response observed in the looming data of full-term infants with increasing age can be largely attributed to the rapid ongoing neuronal specialization in the brain during the first years of infancy (Paus et al., 2001; Mukherjee et al., 2002; Dubois et al., 2006). An increasing number of researchers agree on the notion of experience-specific specialization of neuronal networks and pathways, where given cortical regions become increasingly selective in their response properties, and processing speed increases with an individual's experience with different environmental stimuli (Mukherjee et al., 2002; Dubois et al., 2006; Agyei et al., 2014). Researchers have found that the fiber

volume of white matter increases during early infancy until adulthood due to ongoing axonal myelination (Paus et al., 2001; Mukherjee et al., 2002; Dubois et al., 2006). Axonal myelination serves to increase the speed of neural communication. Thus, increased myelination may serve as an explanation to why processing speed of important visual information increases with age. This confirms earlier studies on normally developing infants, which have shown that VEP latencies reduce with increasing age, and reach levels close to those of adults during the first years of life (Lodge, Armington, Barnet, Shanks, & Newcomb, 1969; Blom, Barth, & Visser, 1980; Moskowitz & Sokol, 1983).

The analysis of optic flow VEPs also revealed that only full-term infants at 12 months of age discriminated significantly between the three visual motion conditions, with shortest latencies for forwards optic flow, longer latencies for reversed optic flow, and longest latencies for random visual motion. At 4-5 months of age, neither the preterm nor the full-term infants significantly discriminated between the three motion conditions. The significant discrimination between conditions observed in 12-month-old full-term infants can be attributed to the increased experience with self-initiated locomotion (Gilmore & Rettke, 2003; Gilmore et al., 2004). One explanation as to why the forwards optic flow condition had the shortest latencies can be due to the fact that humans typically move in a forward direction while performing everyday tasks. When we walk, crawl and drive, we typically experience that the environment flows towards us, rather than away from us. It is therefore fair to expect that the human brain is most adjusted to receiving forwards optic flow information while navigating through the environment. Thus, we expect the brain to react more rapidly to familiar visual motion stimuli than to more unfamiliar reversed optic flow, which simulates backwards movement through the environment, or random motion, which is a more complex motion pattern seldom experienced in the natural environment of humans. As infants at 4-5 months have a limited repertoire of self-initiated locomotion, their brains have not yet formed specialized networks for the different types of visual motion. This is supported by earlier findings (Van der Meer et al., 2008; Agyei et al., 2014), which indicate that infants process both optic flow and random visual motion significantly slower than adults, but that their speed of visual motion processing, especially for optic flow, increases during the first year of life. Increased neuronal specialization during development can explain why, as infants start crawling and walking and generally experience more self-produced optic flow, the latency of the N2 becomes shorter with age, especially for forwards optic flow.

However, the VEP analysis of optic flow revealed that the preterm infants did not discriminate between the three visual motion conditions, neither at 4-5 nor at 12 months. In addition, the preterm infants did not show a significant decrease in VEP latencies in the optic flow experiment, and did not show a significant decrease in time-to-collision of their looming-related VEP responses in the looming experiment. These findings could be indicative of a dorsal stream deficit caused by preterm birth. Long N2 latencies and earlier looming-related VEP responses could possibly indicate a lack of specialized networks for rapid motion processing in preterm infants. Individual analyses carried out on VEP data for optic flow in order to investigate whether any of the preterm infants showed abnormally high VEP latencies pointed to three preterm infants who showed extremely long latencies for both forwards and reversed optic flow, and an additional two preterm infants who showed extremely long latencies for forwards optic flow only.

VEP analysis of looming data revealed that only the full-term infants at 12 months seemed to time their looming-related VEP responses to a fixed time-to-collision. This indicates that they were using a strategy based on time when timing their brain responses to the looming object on a direct collision course. This confirms earlier findings, showing that full-term infants tend to switch from a less efficient to a more efficient timing strategy with age (Kayed & Van der Meer, 2000, 2007; Van der Meer et al., 2012). The preterm infants, however, seemed to be using a strategy based on visual angle, holding the visual angle constant, thus resulting in different response times based on the looming condition. A strategy based on visual angle may pose a challenge as it is less efficient and can lead to a response occurring too early or too late, depending on the size of the selected visual angle and the acceleration of the loom (Kayed & Van der Meer, 2000). Incorrect timing of a response to an object on a collision course may further indicate poor prospective control (Van der Meer et al., 1994; Van der Meer, Van der Weel, Lee, Laing, & Lin, 1995).

As expected based on a visual angle strategy, the average looming-related VEP responses for preterm infants occurred closer to the time of collision in the 2s loom sequence than in the 3s and 4s loom sequences. Longest time-to-collision was observed in the 4s loom sequence. The individual analysis of looming VEPs was based on the standard deviations between the three looming conditions, rather than the means of the looming conditions separately, as high standard deviations indicate that the averaged looming-related VEP responses are distant from the mean, thus indicating that the infant is not using a timing

strategy based on time. Three preterm infants stood out with their extremely high standard deviations.

TSE analysis of optic flow and looming data revealed that full-term infants show an increasing amount of synchronized activity in the late alpha and early beta frequencies with increasing age when processing visual motion information. The desynchronization in theta band frequencies observed in both groups of infants in both testing sessions in accordance with earlier research (Van der Meer et al., 2008; Van der Weel & Van der Meer, 2009; Agyei et al., 2014) showing that EEG in younger infants is dominated by low-frequency activity after being presented with visual motion stimuli. Low frequencies are typically associated with higher amplitudes and an increase in the number of coherently activated neurons (Pfurtscheller & Da Silva, 1999), while desynchronization has been shown to occur following a novel and complex stimulus and is a sign of neurons preparing to process sensory information (Boiten et al., 1992; Pfurtscheller, 1992).

The increase of higher-frequency synchronized activity in full-term infants with age confirms earlier research (Agyei et al., 2014), showing that healthy, full-term infants at 11-12 months show induced brain activity as a function of visual motion more similar to that found in adults (Van der Meer et al., 2008). This could be an indication that as infants grow older, there is a progression from larger, less specialized cell assemblies, to a more mature pattern of specialization in processing visual motion including fewer but more specialized neurons. The appearance of synchronized activity could be indicative of a shift in cortical coupling, where a slower theta-band frequency communication network is gradually replaced by more effective cortical coupling using synchronized high-frequency activity when processing visual motion stimuli, as proposed by Agyei et al. (2014).

Similar results were observed in the frequency analysis of the looming experiment, where the TSEs of the combined looming condition for both full-term and preterm infants at 4-5-months of age were dominated by both synchronized and desynchronized activity in the theta and early alpha frequency range. At 12 months of age, the full-term infants showed an increase in synchronized activity in higher frequency ranges, indicating a rearrangement of neural networks, with fewer, more specialized neurons allowing faster processing of looming stimuli. The appearance of synchronized activity in the TSEs of full-term infants at 12 months of age as a function of both optic flow and looming is in accordance with the significant decrease in VEP latencies and in the time-to-collision of the looming-related VEP responses observed in the analysis of evoked activity. Together, these findings provide evidence that, in

full-term infants, with age and increased self-initiated locomotor experience (Held & Hein, 1963), there indeed has been a development where neurons have become more specialized, and therefore have made visual motion processing more efficient.

Less synchronization in higher frequency bands was observed in the preterm group at 12 months in general, and in the TSE of the motion condition in the optic flow experiment, three preterm infants showed little to no synchronization in late alpha and/or early beta. This was confirmed by a bootstrapping procedure, showing no significant differences in high frequency synchronization when the motion condition was compared to the static condition. Similar results were observed in the TSE of the combined looming condition, where two preterm infants showed little to no synchronization in late alpha and/or early beta frequencies.

The lack of high-frequency activity observed in preterm infants at 12 months of age, in combination with the longer VEP latencies and longer time-to-collision in the looming-related VEPs, indicates that the preterm infants have not yet developed sufficiently specialized networks for rapid processing of visual motion information. These findings are in conjunction with past studies, which have found that preterm infants have less myelinated cortical white matter (Hüppi et al., 1998; Mewes et al., 2006), and demonstrate slower cortical growth (Kapellou et al., 2006) than their full-term peers.

Problems with processing visual motion information efficiently can lead to missteps and accidents, portraying the individual as "clumsy". Clumsy children have in later years been placed in the diagnostic category of developmental coordination disorder (DCD) (Holsti, Grunau, & Whitfield, 2002). According to the American Psychiatric Association (1994, as cited in Holsti et al., 2002), children with DCD have poorer performance in daily activities that require motor coordination. DCD is not caused by a general medical condition such as cerebral palsy, hemiplegia, or muscular dystrophy, and cannot be accounted for by a known physical illness or injury (American Psychiatric Association, 1994, as cited in Holsti et al., 2002). Several studies indicate that DCD is more prevalent amongst preterm infants, and that the minor motor disabilities persist despite improvements in care (Holsti et al., 2002; Foulder-Hughes & Cooke, 2003; Davis, Ford, Anderson, & Doyle, 2007; Goyen & Lui, 2009).

Poor performance on motor tasks not accounted for by any general medical condition can be attributed to poor visual motion processing, as being able to perceive motion correctly is essential in in the control of walking direction (Warren et al., 2001; Bruggeman et al., 2007), postural adjustment, time-to-collision calculations (Van der Meer et al., 1994; Kayed & Van der Meer, 2009), and obstacle avoidance (Wilkie & Wann, 2003). Problems with

processing visual motion information, a dorsal stream function, have been found in a number of developmental disorders associated with poor performance on motor tasks, including developmental dyspraxia, hemiplegia (Gunn et al., 2002; Braddick et al., 2003; Grinter et al., 2010), and autism spectrum disorders (Spencer et al., 2000). In addition, research indicates that infants and children born preterm show impairment in, or a delay in the development of, visual motion processing (Van Braeckel et al., 2008; Guzzetta et al., 2009; Atkinson & Braddick, 2012; Tremblay et al., 2014). Problems with processing visual motion may serve as an explanation as to why individuals born preterm more often show neurodevelopmental impairments. One could expect that, when age is corrected for prematurity, preterm infants would follow a developmental path similar to that of full-term infants. However, in conjunction with earlier findings, the results of the current study indicate that preterm infants do not show the same development in visual motion processing as seen in full-term infants, which could be indicative of a dorsal stream deficit.

Differences in dorsal stream functions, but not in ventral stream functions, have been found between preterm and full-term infants (Hammarrenger et al., 2007; Tremblay et al, 2014). The dorsal visual stream is found to develop earlier and mature more rapidly than the ventral visual stream, and is therefore more prone to be disrupted by the effects of preterm birth. Hammarrenger et al. (2003) found that VEP amplitudes in the dorsal stream elicited by different contrast stimuli reached a ceiling at around 25 weeks after birth in healthy, full-term infants, slowly leveling off during the remaining weeks of the first year. As amplitudes reflect the number of coherently activated neurons (Pfurtscheller & Lopes da Silva, 1999), a decrease in amplitudes could be indicative of an increased specialization in the brain. VEP amplitudes can be difficult to measure in the infant brain due to the infants' relatively thin skulls (Grieve, Emerson, Fifer, Isler, & Stark, 2003), but latencies have proven to be useful when indicating brain development as a function of synapse production and specialization (Van der Meer et al., 2012; Agyei et al., 2014). The latencies of VEPs decreased significantly with age for the full-term infants, indicating brain plasticity and efficient specialization of neuronal networks (Paus et al., 2001; Mukherjee et al., 2002; Dubois et al., 2006). As the preterm infants did not show such a development, and continued to show long VEP latencies as a function of visual motion stimuli at 12 months, this could be indicative of a lack of specialization in, and development of, the dorsal visual stream.

A dorsal stream vulnerability leading to difficulties in processing visual motion can have a number of implications for preterm infants' development. As mentioned above,

processing visual motion information is crucial in a number of everyday tasks, and when this processing is impaired, children are often referred to as "clumsy". The fact that studies investigating VEPs can be used to uncover dorsal stream deficits before the possible onset of symptoms of perceptuo-motor anomalies (Hammarrenger et al., 2007; Tremblay et al., 2014) suggests that early diagnosis and intervention can be made more available in the future. As an increasing number of studies indicate that preterm infants have a dorsal stream vulnerability, these findings can possibly help parents, kindergartens and schools facilitate preterm infants so as to minimize the effects of abnormal visual motion processing. In addition, future research may reveal if the use of visual motion experiments in young infants can help pointing out individuals who have a greater impairment in dorsal stream functions. In this study, the same two preterm infants stood out in three of four analyses based on individual data, where they showed extremely long optic flow-related VEP latencies for optic flow stimuli, outlier values based on standard deviations of their looming-related VEPs for the three looming conditions, as well as a lack of high-frequency activity in the frequency analyses. As their current neurological status is unknown to the experimenter, a follow-up study when the infants reach school age would be of interest to investigate whether these infants still have impaired dorsal stream-related functions, and whether this affects their everyday lives.

In conclusion, the present study found that, with age, full-term infants increase their sensitivities to optic flow, and become capable of detecting structured optic flow more efficiently than random visual motion. In addition, full-term infants significantly decreased their looming-related VEP responses with age, and responded at a fixed time-to-collision at 12 months of age, indicating that they were using a timing strategy based on time. Frequency analyses revealed an appearance of high-frequency synchronized induced brain activity at 12 months of age in full-term infants. This is indicative of increased specialization and myelination of the normally developing infant brain with age. However, the preterm infants did not show a similar progression when it comes to the processing of visual motion with age. The preterm infants did not decrease their VEP latencies with age in the optic flow experiment and did not become capable of detecting structured optic flow more efficiently than random visual motion. In addition, the preterm infants did not decrease the time-to-collision of their looming-related VEP responses with age, and seemed to be using a less efficient timing strategy based on the looming object's visual angle at 12 months of age. Frequency analyses showed less high-frequency synchronized activity in the preterm infants at 12 months of age compared to the full-term infants, and some preterm infants did not show

any high-frequency synchronized activity at all. These results reveal that preterm infants do not show the same development in visual motion processing as full-term infants, and supports the notion of dorsal stream impairment caused by premature birth. Future studies with larger sample sizes, as well as follow-up studies of the preterm infants enrolled in the present study at school age may reveal whether there truly is an impairment of dorsal stream-related functions in preterm infants, whether the dorsal stream vulnerability persists into later life, and what potential effects this may have on the children's everyday lives.

References

Adolph, K. E., Eppler, M. A., Marin, L., Weise, I. B., & Clearfield, M. W. (2000). Exploration in the service of prospective control. *Infant Behavior and Development, 23,* 441-460.

Agyei, S. B., Holth, M., Van der Weel, F. R., & Van der Meer, A. L. H. (2014). Longitudinal study of perception of structured optic flow and random visual motion in infants using high-density EEG. *Developmental Science, 18*(3), 436-451.

Andersen, R. A. (1997). Neural mechanisms of visual motion perception in primates. *Neuron, 18,* 865-872.

Atkinson, J., & Braddick, O. (2012). Visual and visuocognitive development of children born very prematurely. Preedy, V. R. (Red.), *Handbook of Growth and Growth Monitoring in Health and Disease* (pp. 543-656). New York: Springer.

Blom, J. L., Barth, P. G., & Visser, S. L. (1980). The visual evoked potential in the first six years of life. *Electroencephalography and Clinical Neurophysiology, 48,* 395-405.

Boiten, F., Sergeant, J., & Geuze, R. (1992). Event-related desynchronization: The effects of energetic and computational demands. *Electroencephalography and Clinical Neurophysiology, 82*(4), 302-309.

Braddick, O., Atkinson, J., & Wattam-Bell, J. (2003). Normal and anomalous development of visual motion processing: Motion coherence and "dorsal-stream vulnerability". *Neuropsychologia, 41,* 1769-1984.

Bruce, V., Green, P. R., & Georgeson, M. A. (2003). *Visual Perception: Physiology, Psychology and Ecology 4th Ed*. New York, NY: Psychology Press.

Bruggeman, H., Zosh, W., & Warren, W. H. (2007). Optic flow drives human visuo-locomotor adaptation. *Current Biology, 17,* 2035-2040.

Counsell, S. J., Edwards, A. D., Chew, A. T. M., Anjari, M., Dyet, L. E., Srinivasan, L., Boardman, J. P., Allsop, J. M., Hajnal, J. V., Rutherford, M. A., & Cowan, F. M. (2008). Specific relations between neurodevelopmental abilities and white matter microstructure in children born preterm. *Brain, 131,* 3201-3208.

Davis, N. M., Ford, G. W., Anderson, P. J., & Doyle, L. W. (2007). Developmental coordination disorder at 8 years of age in a regional cohort of extremely-low-birthweight or preterm infants. *Developmental Medicine & Child Neurology, 49*(5), 325-330.

De Jong, B. M., Shipp, S., Skidmore, B., Frackowiak, R. S. J., & Zeki, S. (1994). The cerebral activity related to the visual perception of forward motion in depth. *Brain, 117,* 1039-1054.

Di Russo, F., Martínez, A., Sereno, M. I., Pitzalis, S., & Hillyard, S. A. (2002). Cortical sources of the early components of the visual evoked potential. *Human Brain Mapping, 15*(2), 95-111.

Dubois, J., Hertz-Pannier, L, Dehaene-Lambertz, G., Cointepass, Y., & Le Bihan, D. (2006). Assessment of the early organization and maturation of infants' cerebral white matter fiber bundles: A feasibility study using quantitative diffusion tensor imaging and tractography. *NeuroImage, 30,* 1121-1132.

Edelman, G. M. (1993). Neural Darwinism: Selection and reentrant signaling in higher brain function. *Neuron, 10*, 115-125.

Feree, T. C., Luu, P., Russell, G. S., & Tucker, D. M. (2001). Scalp electrode impedance, infection risk, and EEG data quality. *Clinical Neurophysiology, 112,* 536-544.

Fesi, J. D., Thomas, A. L., & Gilmore, R. O. (2014). Cortical responses to optic flow and motion contrast across patterns and speeds. *Vision Research, 100,* 56-71.

Field, A. (2009). *Discovering Statistics Using SPSS* (3rd Ed.). London: SAGE Publications Ltd.

Foulder-Hughes, L. A., & Cooke, R. W. I. (2003). Motor, cognitive, and behavioral disorders in children born very pre-term. *Developmental Medicine and Child Neurology*, *45,* 97-103.

Gibson, J. J. (1986). *The Ecological Approach to Visual Perception*. Hillsdale, NJ: Lawrence Erlbaum Associates, Inc.

Gilmore, R. O., Baker, T. J., & Grobman, K. H. (2004). Stability in young infants' discrimination of optic flow. *Developmental Psychology, 40*(2), 259-270.

Gilmore, R. O., Hou, C., Pettet, M. W., & Norcia, A. M. (2007). Development of cortical responses to optic flow. *Visual Neuroscience, 24,* 845-856.

Gilmore, R. O., & Rettke, H. J. (2003). Four-month-olds' discrimination of optic flow patterns depicting different directions of observer motion. *Infancy, 4*(2), 177-200.

Goyen, T.-A., & Lui, K. (2009). Developmental coordination disorder in «apparently normal» schoolchildren born extremely preterm. *Archives of Disease in Childhood, 94,* 298-302.

Grieve, P. G., Emerson, R. G., Fifer, W. P., Isler, J. R., & Stark, R. I. (2003). Spatial correlation of the infant and adult electroencephalogram. *Clinical Neurophysiology, 114*(9), 1594-1608.

Grinter, E. J., Maybery, M. T., & Badcock. (2010). Vision in developmental disorders: Is there a dorsal stream deficit? *Brain Research Bulletin, 82,* 147-160.

Gunn, A., Cory, E., Atkinson, J., Braddick, O., Wattam-Bell, J., Guzzetta, A., & Cioni, G. (2002). Dorsal and ventral stream sensitivity in normal development and hemiplegia. *Cognitive Neuroscience and Neuropsychology, 13*(6), 843-847.

Guzzetta, A., Tinelli, F., Del Viva, M. M., Bancale, A., Arrighi, R., Pascale, R. R., & Cioni, G. (2009). Motion perception in preterm children: Role of prematurity and brain damage. *NeuroReport, 20,* 1339-1343.

Haith, M. M. (1966). The response of the human newborn to visual movement. *Journal of Experimental Child Psychology, 3*(3), 235-243.

Hammarrenger, B., Leporé, F., Lippé, S., Labrosse, M., Guillemot, J-P., & Roy, M.-S. (2003). Magnocellular and parvocellular developmental course in infants during the first year of life. *Documenta Ophthalmologica, 107,* 225-233.

Hammarrenger, B., Roy, M.-S., Ellemberg, D., Labrosse, M., Orquin, J., Lippe, S., & Lepore, F. (2007). Developmental delay and magnocellular visual pathway function in very-low-birthweight preterm infants. *Developmental Medicine and Child Neurology, 49*(1), 28-33.

Held, R., & Hein, A. (1963). Movement-produced stimulation in the development of visually guided behavior. *Journal of Comparative and Physiological Psychology, 56*(5), 872-876.

Holliday, I. E., & Meese, T. S. (2005). Neuromagnetic evoked responses to complex motions are greatest for expansion. *International Journal of Psychophysiology, 55,* 145-157.

Holsti, L., Grunau, R. V. E., & Whitfield, M. F. (2002). Developmental coordination disorder in extremely low birth weight children at nine years. *Developmental and Behavioral Pediatrics, 23*(1), 9-15.

Hüppi, P. S., Maier, S. E., Peled, S., Zientara, G. P., Barnes, P. D., Jolesz, F. A., & Volpe, J. J. (1998). Microstructural development of human newborn cerebral white matter assessed in vivo by diffusion tensor magnetic resonance imaging. *Pediatric Research, 44,* 584-590.

Johnson, M. H. (2000). Functional brain development in infants: Elements of an interactive specialization framework. *Child Development, 71*(1), 75-81.

Jongmans, M., Mercuri, E., De Vries, L., Dubowitz, L., & Henderson, S. E. (1997). Minor neurological signs and perceptual-motor difficulties in prematurely born children. *Archives of Disease in Childhood, 76,* F9-F14.

Kapellou, O., Counsell, S. J., Kennea, N., Dyet, L., Saeed, N., Stark, J., Maalouf, E., Duggan, P., Ajayi-Obe, M., Hajnal, J., Allsop, J. M., Boardman, J., Rutherford, F. C., & Edwards, A. D. (2006). Abnormal cortical development after premature birth shown by altered allometric scaling of brain growth. *PLoS ONE, 3*(8), 1382-1390.

Kayed, N. S., Farstad, H., & Van der Meer, A. L. H. (2008). Preterm infants' timing strategies to optical collisions. *Early Human Development, 84,* 381-388.

Kayed, N. S., & Van der Meer, A. L. H. (2000). Timing strategies used in defensive blinking to optical collisions in 5- to 7-month-old infants. *Infant Behavior and Development, 23,* 253-270.

Kayed, N. S., & Van der Meer, A. L. H. (2007). Infants' timing strategies to optical collisions: A longitudinal study. *Infant Behavior and Development, 30,* 50-59.

Kayed, N. S., & Van der Meer, A. L. H. (2009). A longitudinal study of prospective control in catching by full-term and pre-term infants. *Experimental Brain Research, 194,* 245-258.

King, S. M., & Cowey, A. (1992). Defensive responses to looming visual stimuli in monkeys with unilateral striate cortex ablation. *Neuropsychologia,30*(11), 1017-1025.

Larroque, B., Ancel, P.-Y., Marnet, S., Marchland, L., André, M., Annaud, C., Pierrat, V., Rozé, J.-C., Messer, J., Thiriez, J., Burguet, A., Picaud, J.-C., Bréart, G., & Kaminski, M. (2008). Neurodevelopmental disabilities and special care of 5-year-old children born before 33 weeks of gestation (the EPIPAGE study): A longitudinal cohort study. *The Lancet, 371,* 813-820.

Lodge, A., Armington, J. C., Barnet, A. B., Shanks, B. L., & Newcomb, C. N. (1969). Newborn infants' electroretinograms and evoked electroencephalographic responses to orange and white light. *Child Development, 40*(1), 267-293.

Luck, S. J. (2005). *An Introduction to the Event-Related Potential Technique*. Cambridge, MA: MIT Press.

Markestad, T., & Halvorsen, B. (2007). Faglige retningslinjer for oppfølging av for tidlig fødte barn. *Sosial- og helsedirektoratet,* 17-23.

Martinussen, M., Fischl, B., Larsson, H. B., Skranes, J., Kulseng, S., Vangberg, T. R., Vik, T., Brubakk, A.-M., Haraldseth, O., & Dale, A. M. (2005). Cerebral cortex thickness in 15-year-old adolescents with low birth weight measured by automated MRI-based method. *Brain, 128,* 2588-2596.

Mewes, A. U. J., Hüppi, P. S., Als, H., Rybicki, F. J., Inder, T. E., McAnulty, G. B., Mulkern, R. V., Robertson, R. L., Rivkin, M. J., & Warfield, S. K. (2006). Regional brain development in serial magnetic resonance imaging of low-risk preterm infants. *Pediatrics, 118*(1), 23-33.

Morrone, M. C., Tosetti, M., Montanaro, D., Fiorentini, A., Cioni, G., & Burr, D. C. (2000). A cortical area that responds specifically to optic flow revealed by fMRI. *Nature Neuroscience, 3*(12), 1322-1328.

Moskowitz, A., & Sokol, S. (1983). Developmental changes in the human visual system as reflected by the latency of the pattern reversal VEP. *Electroencephalography and Clinical Neurophysiology, 56,* 1-15.

Mukherjee, P., Miller, J. H., Shimony, J. S., Philip, J. V., Nehra, D., Snyder, A. Z., Conturo, T. E., Neil, J. J., & McKinstry, R. C. (2002). Diffusion-tensor MR imaging of gray and white matter development during normal human brain maturation. *American Journal of Neuroradiology, 23,* 1445-1456.

Náñez, J. E. (1988). Perception of impending collision in 3-to 6-week-old human infants. *Infant Behavior and Development, 11,* 447-463.

Nosarti, C., Al-Asady, M. H. S., Frangou, S., Stewart, A. L., Rifkin, L., & Murray, R. M. (2002). Adolescents who were born very preterm have decreased brain volumes. *Brain, 125,* 1616-1623.

Parrish, E. E., Giaschi, D. E., Boden, C., & Dougherty, R. (2005). The maturation of form and motion perception in school age children. *Vision Research, 45,* 827-837.

Paus, T., Collins, D. L., Evans, A. C., Leonard, G., Pike, B., & Zijdenbos, A. (2001). Maturation of white matter in the human brain: A review of magnetic resonance studies. *Brain Research Bulletin, 54*(3), 255-266.

Pfurtscheller, G. (1992). Event-related synchronization (ERS): An electrophysiological correlate of cortical areas at rest. *Electroencephalography and Clinical Neurophysiology, 82,* 62-69.

Pfurtscheller, G., & Aranibar, A. (1977). Event-related cortical desynchronization detected by power measurements of scalp EEG. *Electroencephalography and Clinical Neurophysiology, 42,* 817-826.

Pfurtscheller, G., & Lopes da Silva, F. H. (1999). Event-related EEG/MEG synchronization and desynchronization: Basic principles. *Clinical Neurophysiology, 110,* 1842-1857.

Prematur fødsel. (October 31st 2014). In *Store Medisinske Leksikon*. Retrieved from https://sml.snl.no/prematur_f%C3%B8dsel

Probst, Th., Plendl, H., Paulus, W., Wist, E. R., & Scherg, M. (1993). Identification of the visual motion area (area V5) in the human brain by dipole source analysis. *Experimental Brain Research, 93,* 345-351.

Rind, F. C., & Simmons, P. J. (1997). Signaling of object approach by the DCMN neuron of the locust. *Journal of Neurophysiology, 77,* 1029-1033.

Skranes, J., Vangberg, T. R., Kulseng, S., Indredavik, M. S., Evensen, K. A. I., Martinussen, M., Dale, A. M., Haraldseth, O., & Brubakk, A.-M. (2007). Clinical findings and

white matter abnormalities seen on diffusion tensor imaging in adolescents with very low birth weight. *Brain, 130,* 654-666.

Smith, A. T., Wall, M. B., Williams, A. L., & Singh, K. D. (2006). Sensitivity to optic flow in human cortical areas MT and MST. *European Journal of Neuroscience, 23,* 561-569.

Spencer, J., O'Brien, J., Riggs, K., Braddick, O., Atkinson, J., & Wattam-Bell, J. (2000). Motion processing in autism: Evidence for a dorsal stream deficiency. *NeuroReport, 11* (12), 2765-2767.

Sun, H., & Frost, B. J. (1998). Computation of different optical variables of looming objects in pigeon nucleus rotundus neurons. *Nature Neuroscience, 1*(4), 296-303.

Talairach, J., & Tournoux, P. (1988). *Co-Planar Stereotaxic Atlas of the Human Brain*. Stuttgart, Germany: Georg Thieme Verlag.

Tremblay, E., Vannasing, P., Roy, M-S., Lefebvre, F., Kombate, D., Lassonde, M., Lepore, F., McKerral, M., & Gallagher, A. (2014). Delayed early primary visual pathway development in premature infants: High density electrophysiological evidence. *PLoS ONE, 9*(9), 1-9.

Van Braeckel, K., Butcher, P. R., Geuze, R. H., Van Duijn, M. A. J., Bos, A., & Bouma, A. (2008). Less efficient elementary visuomotor processes in 7- to 10-year-old preterm-born children without cerebral palsy: An indication of impaired dorsal stream processes. *Neuropsychology, 22*(6), 755-764.

Van der Meer, A. L. H., Fallet, G., & Van der Weel, F. R. (2008). Perception of structured optic flow and random visual motion in infants and adults: A high-density EEG study. *Experimental Brain Research, 186,* 493-502.

Van der Meer, A. L. H., Svantesson, M., & Van der Weel, F. R. (2012). Longitudinal study of looming in infants with high-density EEG. *Developmental Neuroscience, 34,* 488-501.

Van der Meer, A. L. H., Van der Weel, F. R., & Lee, D. N. (1994). Prospective control in catching by infants. *Perception, 23*(3), 287-302.

Van der Meer, A. L. H., Van der Weel., F. R., Lee, D. N., Laing, I. A., & Lin, J.-P. (1995). Development of prospective control of catching moving objects in preterm at-risk infants. *Developmental Medicine and Child Neurology, 37,* 145-158.

Van der Weel, F. R., & Van der Meer, A. L. H. (2009). Seeing it coming: Infants' brain responses to looming danger. *Die Naturwissenschaften, 96,* 1385-1391.

Wang, Y., & Frost, B. J. (1992). Time to collision is signaled by neurons in the nucleus rotundus of pigeons. *Nature, 356,* 236-238.

Warren, W. H. Jr., Kay, B. A., Zosh, W. D., Duchon, A. P., & Sahuc, S. (2001). Optic flow is used to control human walking. *Nature Neuroscience, 4*(2), 213-216.

Webb, S. J., Long, J. D., & Nelson, C. A. (2005). A longitudinal investigation of visual event-related potentials in the first year of life. *Developmental Science, 8,* 605-616

Wilkie, R. M., & Wann, J. P. (2003). Eye-movements aid the control of locomotion. *Journal of Vision, 3*(11), 677-684.

Yonas, A., Pettersen, L., & Lockman J. J. (1979). Young infants' sensitivity to optical information for collision. *Canadian Journal of Psychology-Revue Canadienne De Psychologie,* 33(4), 268-276.

Yonas, A. (1981). Infants' responses to optical information for collision. In R. N. Aslin, J. R. Alberts, & M. R. Petersen, (Eds.), *Development of Perception: Vol.2. The Visual System,* (pp 313-334). New York: Academic Press.

Appendices

Appendix A

TSE maps across brain regions VClL, PM, and VClR for a) the combined motion condition, b) the static condition, c) when the motion condition is compared to the static dot pattern, and d) the bootstrapping procedure when the motion condition is compared to the static dot pattern in 12-month-old preterm infants DA and EL. Induced desynchronized and induced synchronized activities are shown in blue and red contours, respectively. Epoch is from -200 ms to 800 ms and the frequency is from 4 Hz to 40 Hz.

DA

a)

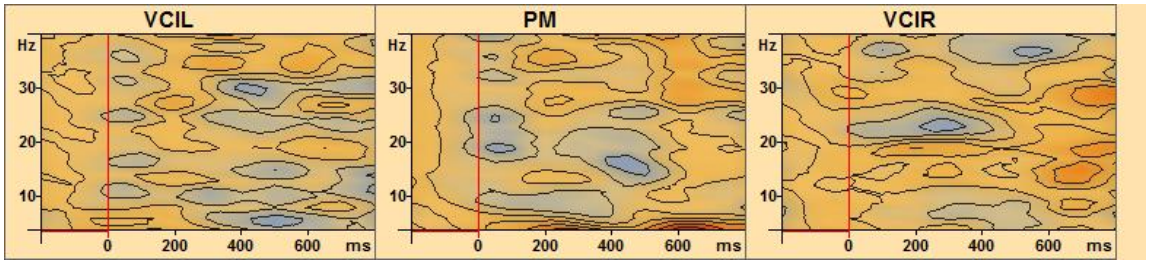

b)

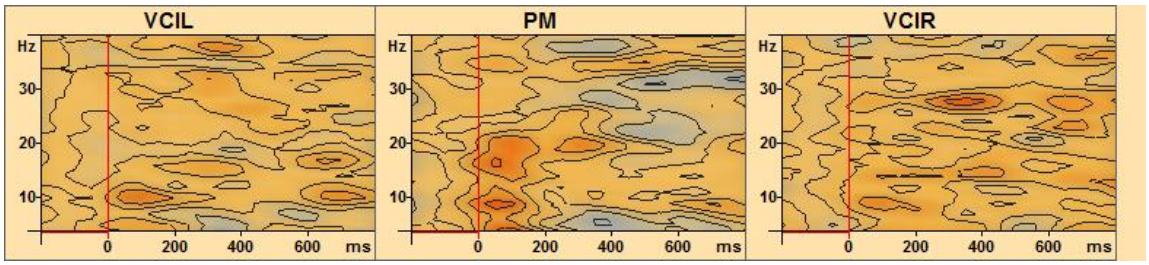

c)

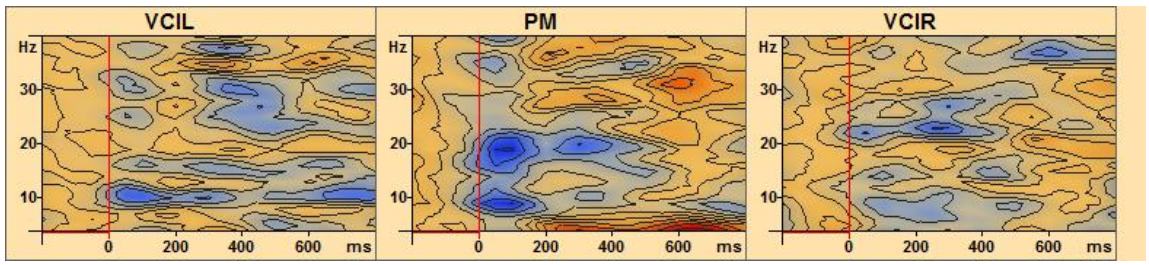

d)

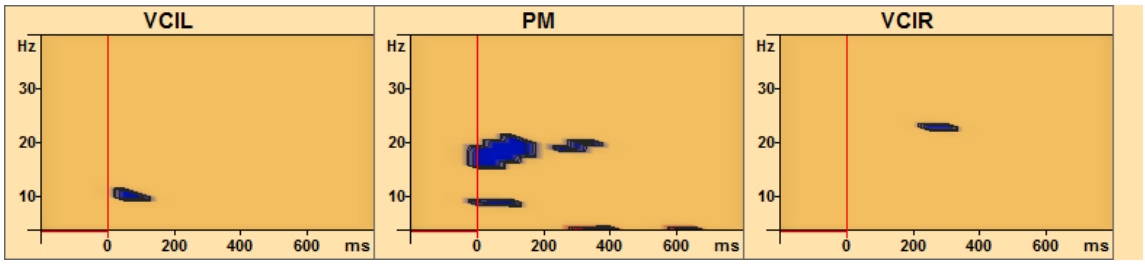

EL

a)

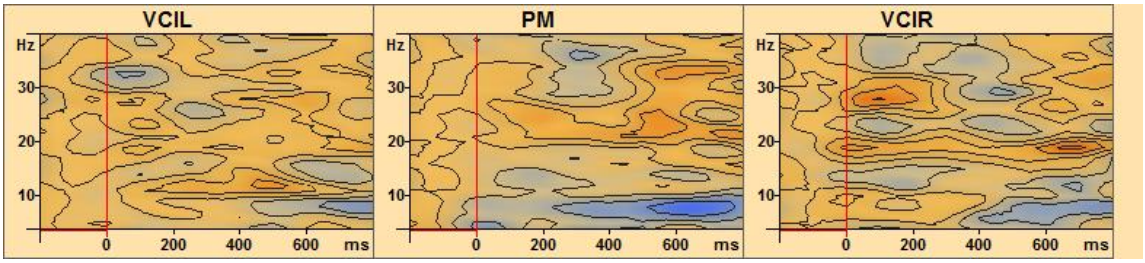
VCIL
PM
VCIR
Hz
30
20
10
0
200
400
600
ms

b)

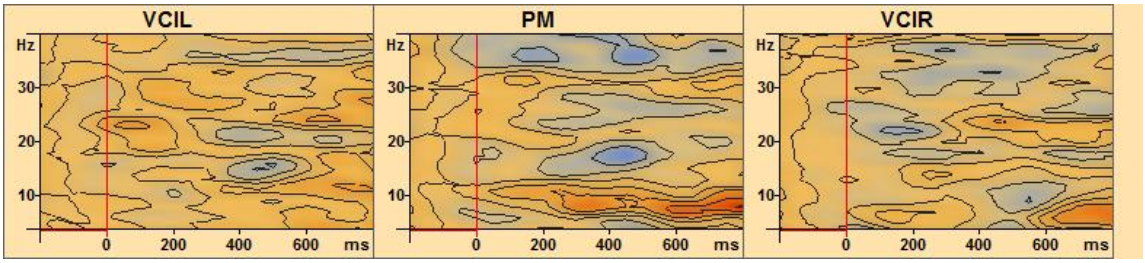
VCIL
PM
VCIR
Hz
30
20
10
0
200
400
600
ms

c)

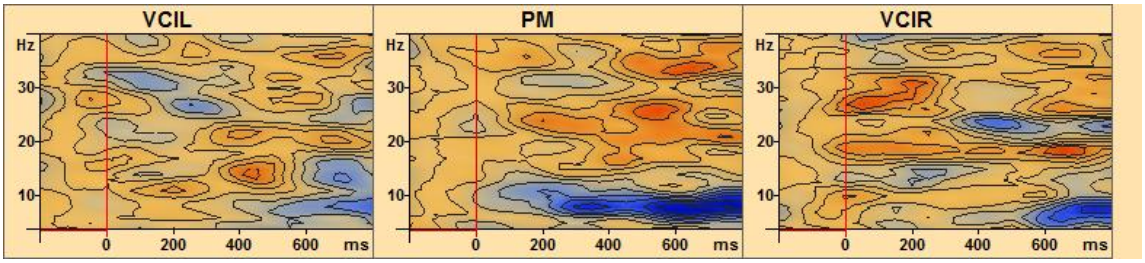
VCIL
PM
VCIR
Hz
30
20
10
0
200
400
600
ms

d)

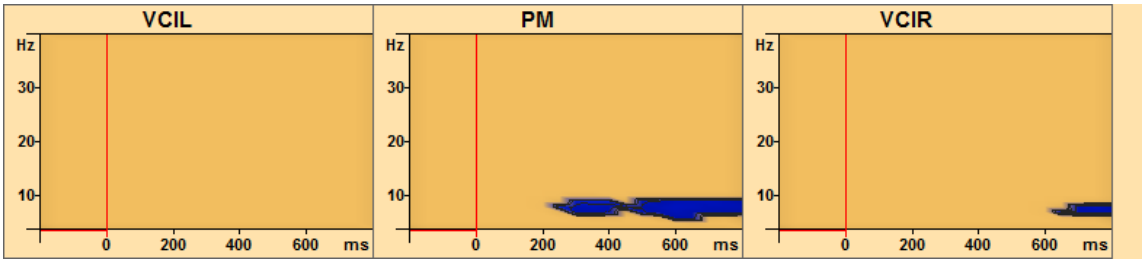
VCIL
PM
VCIR
Hz
30
20
10
0
200
400
600
ms

Appendix B

TSE maps of the combined looming condition across brain regions VCrL, VCvM, and VCrR in 4-5-month-old full-term and preterm infants. Induced desynchronized and induced synchronized activities are shown in blue and red contours, respectively. Epoch is from -300 ms to 300 ms and the frequency is from 4 Hz to 40 Hz.

AK

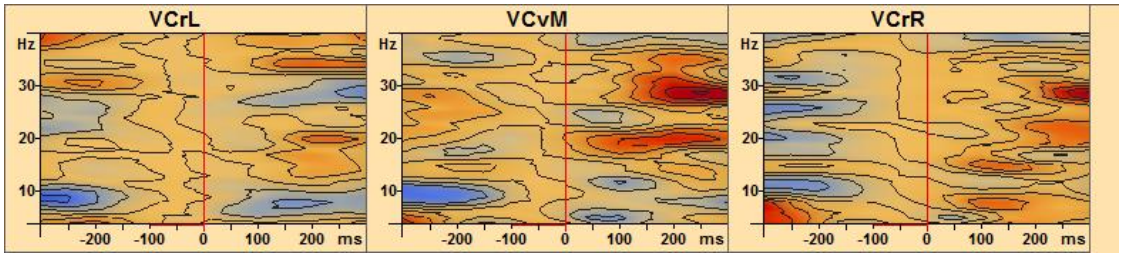

BK

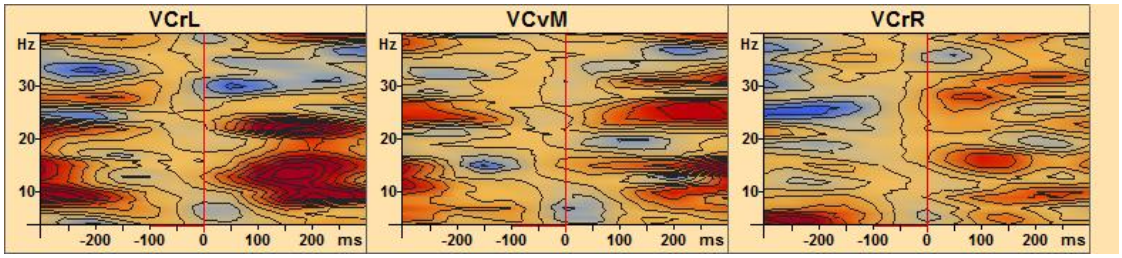

BE

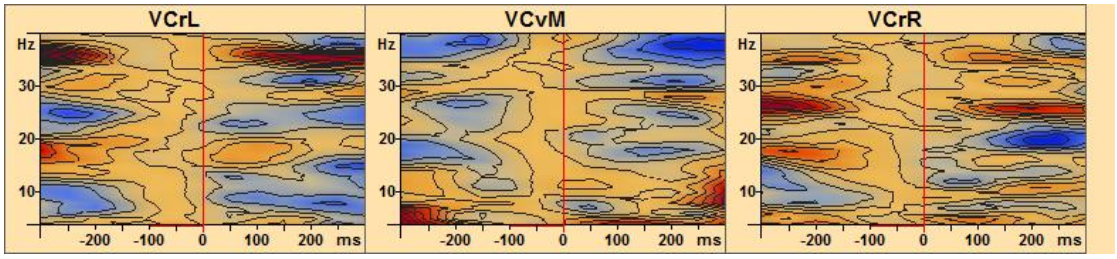

GE

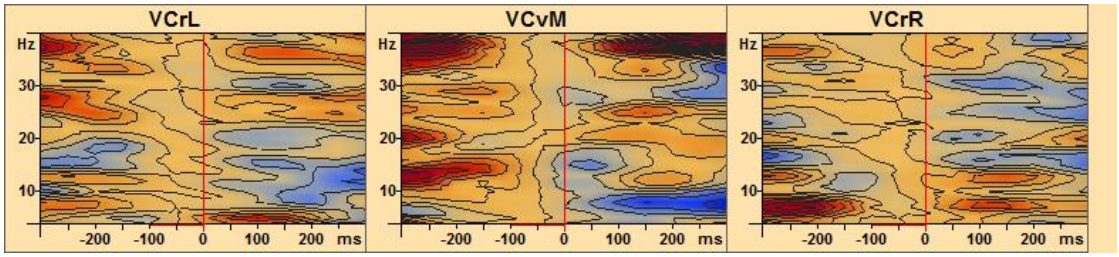

HD

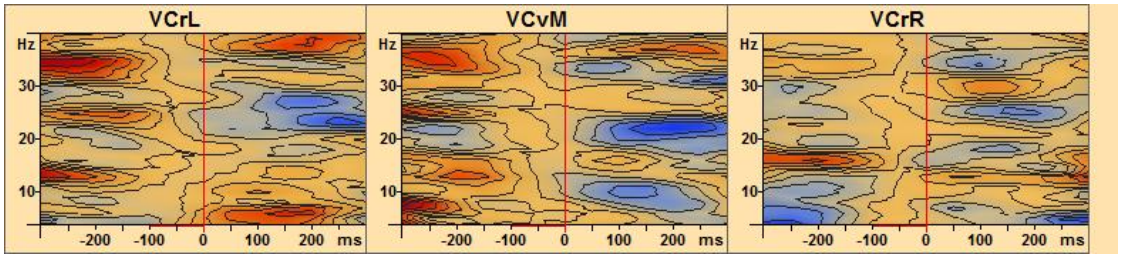

JY

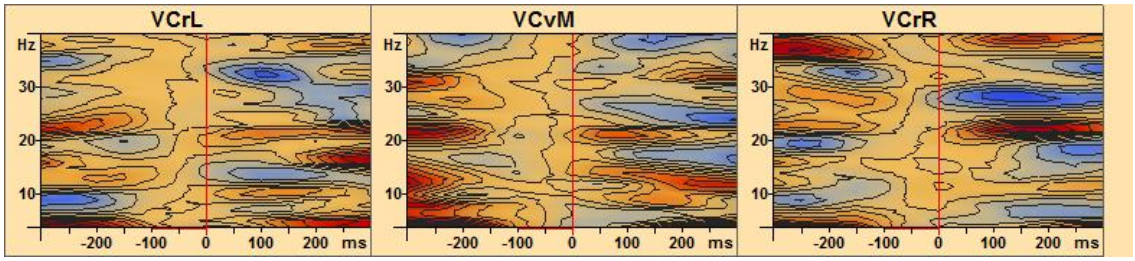

LS

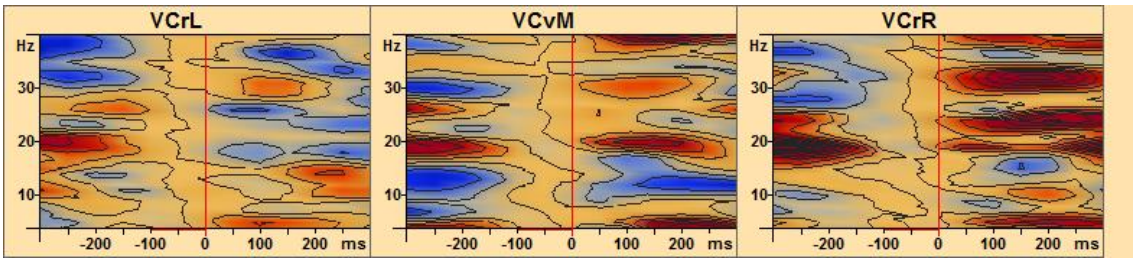

SA

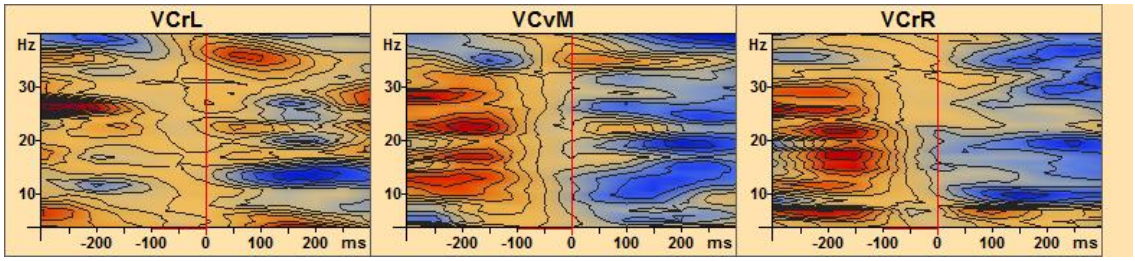

SN

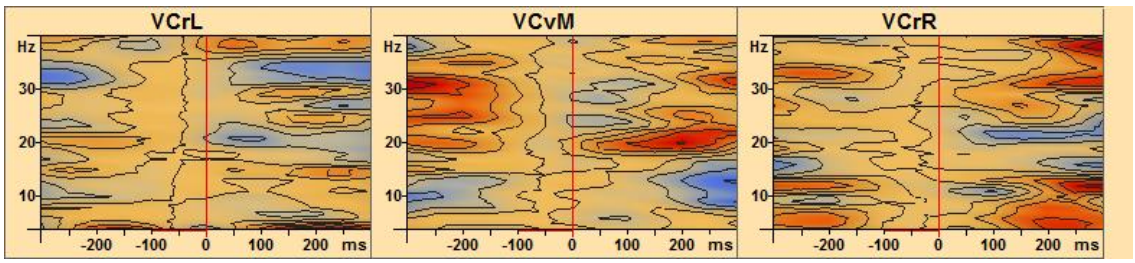

AT

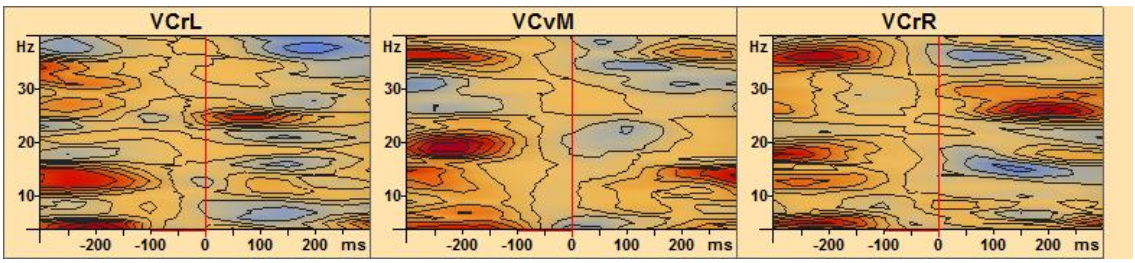

DA

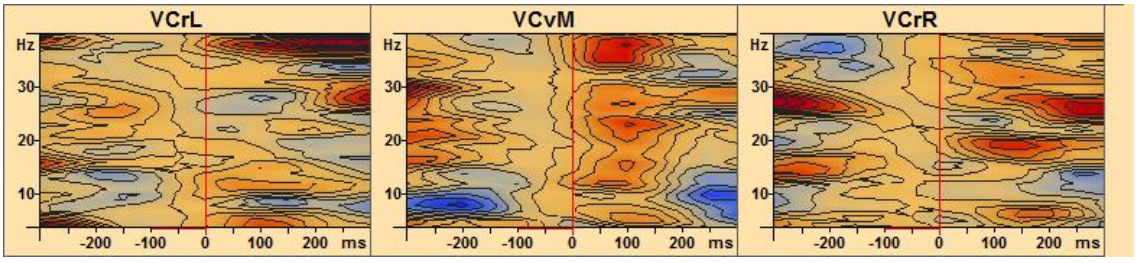

DK

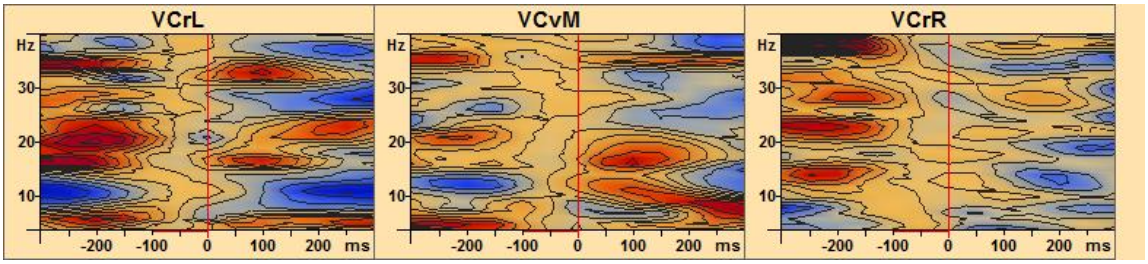

EL

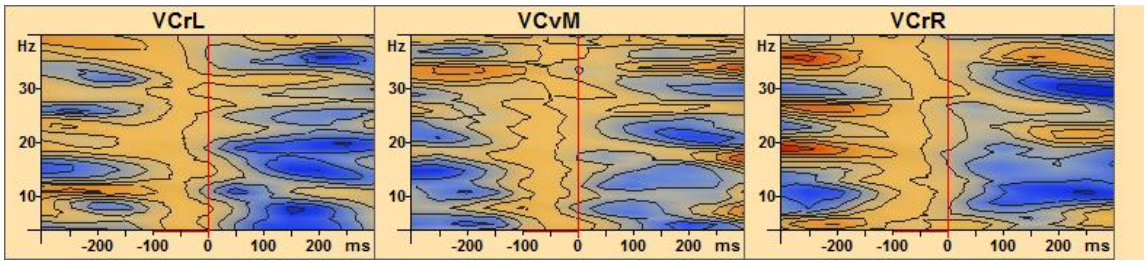

FP

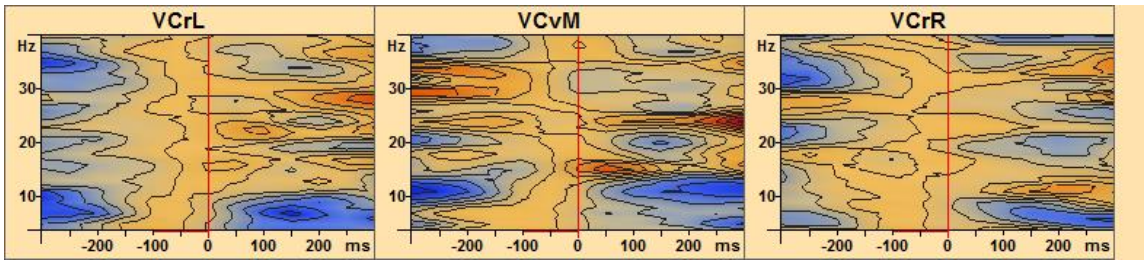

MS

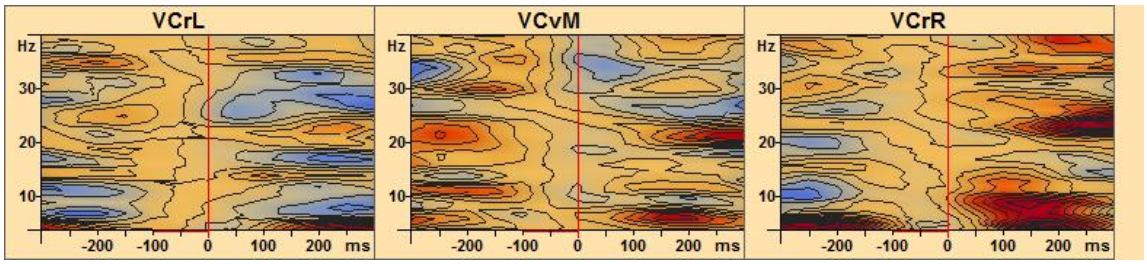

SE

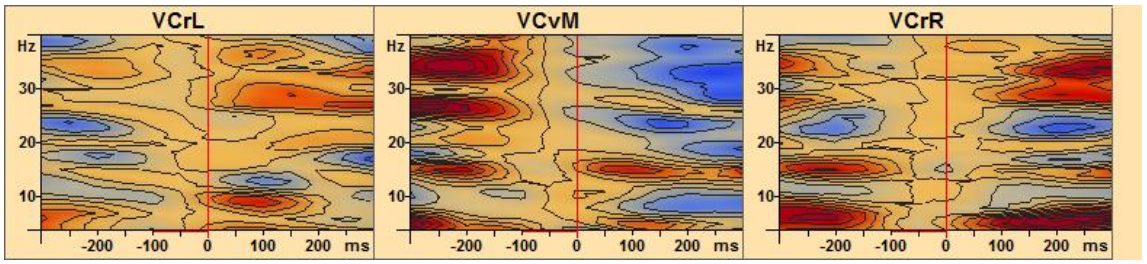

TA

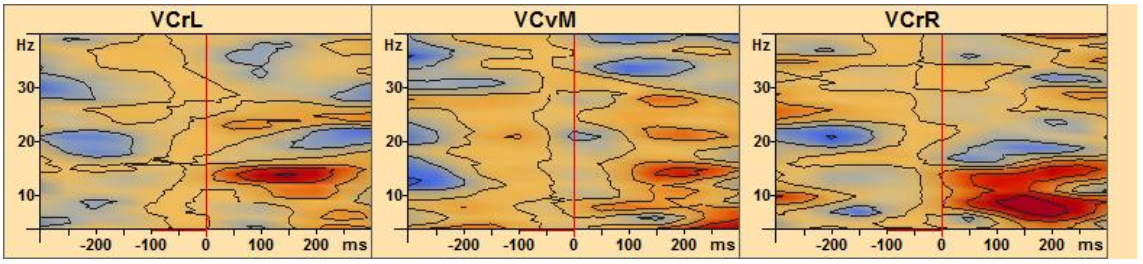

WM

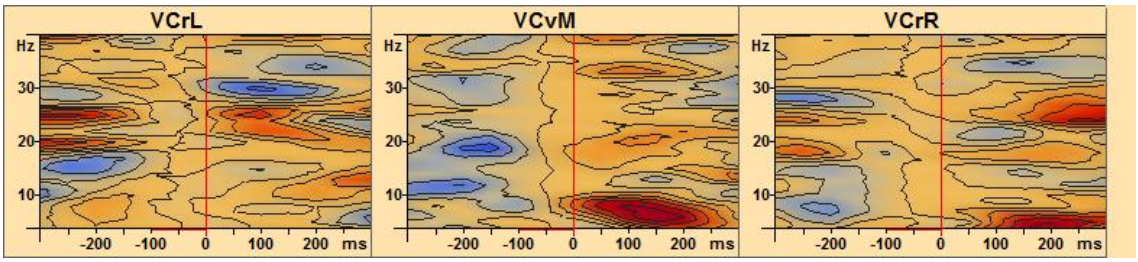

TSE maps of the combined looming condition across brain regions VCrL, VCvM, and VCrR in 12-month-old full-term infants. Induced desynchronized and induced synchronized activities are shown in blue and red contours, respectively. Epoch is from -300 ms to 300 ms and the frequency is from 4 Hz to 40 Hz.

AK

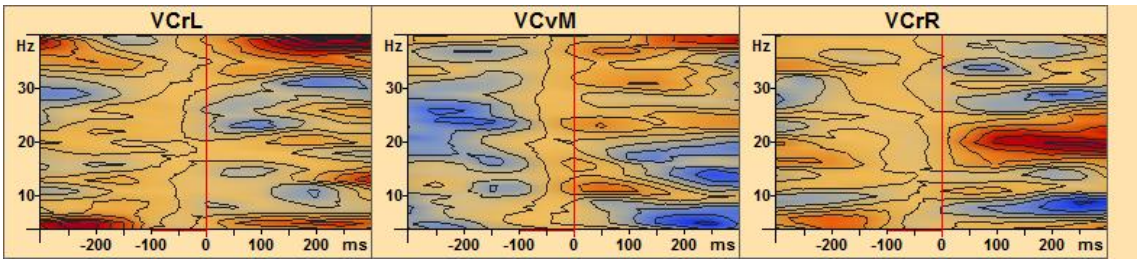

BK

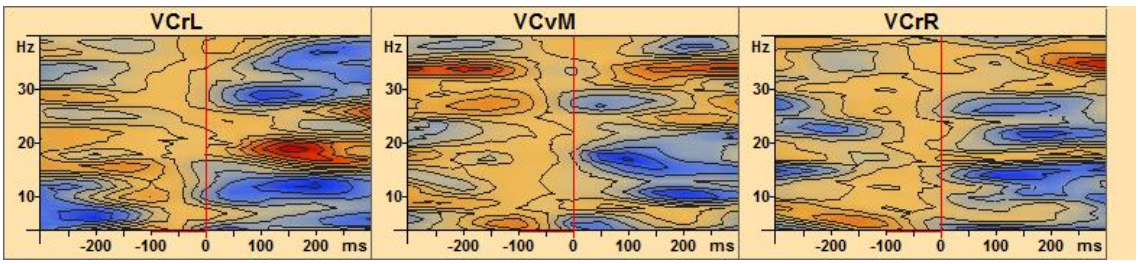

BE

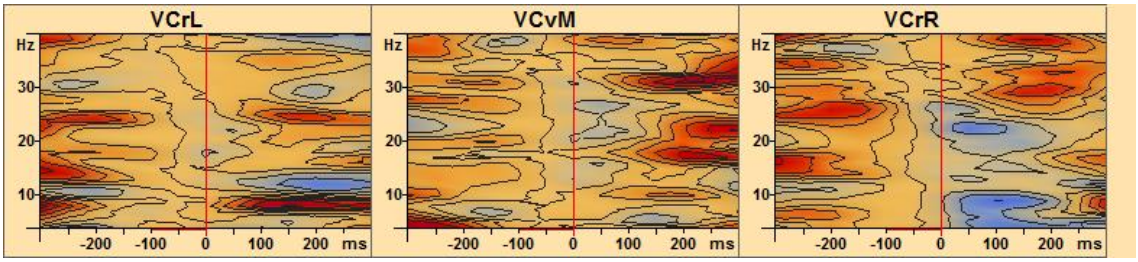

GE

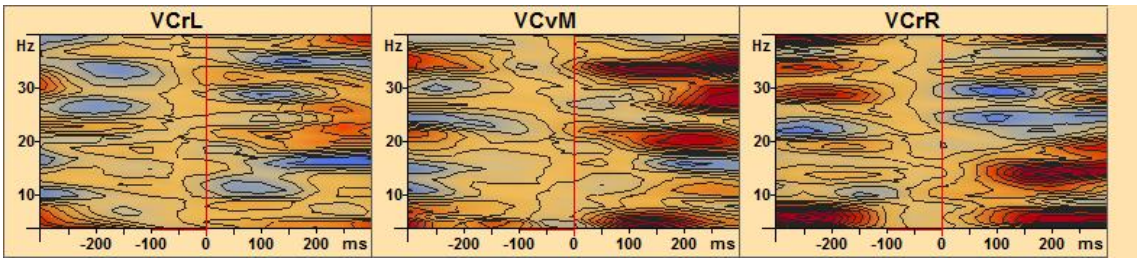

HD

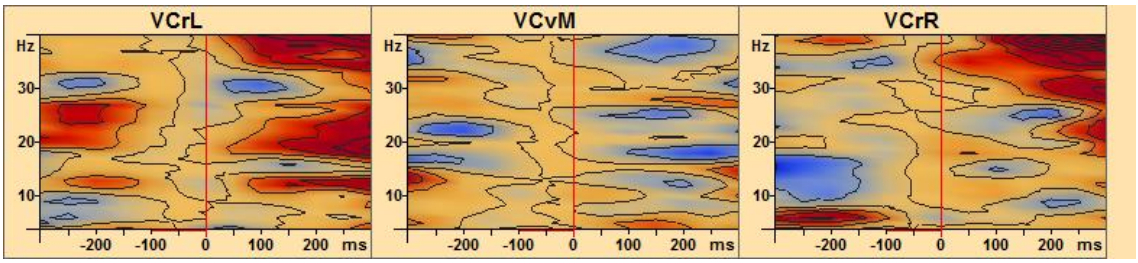

JY

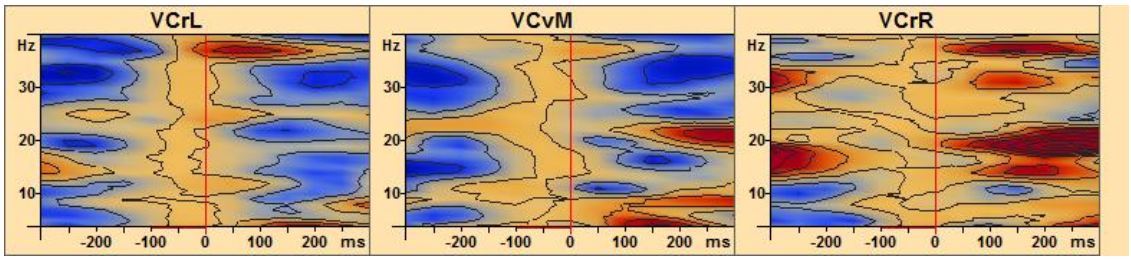

LS

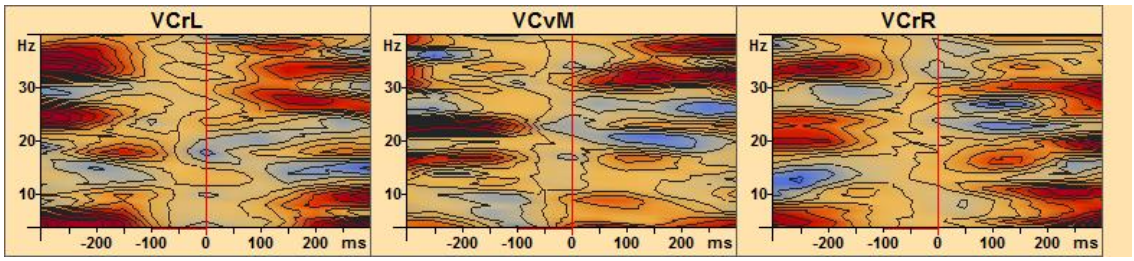

SA

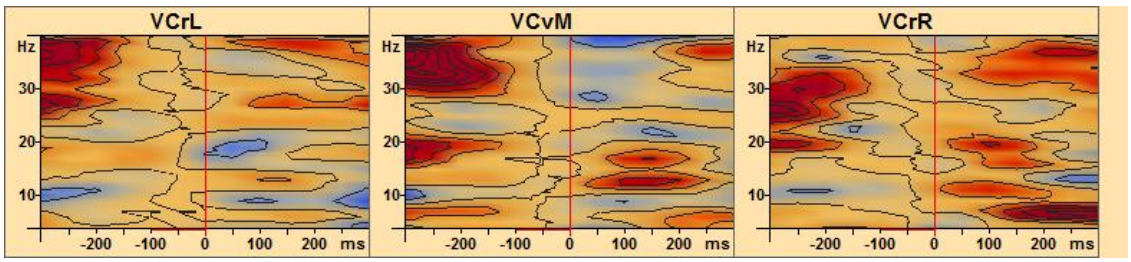

SN

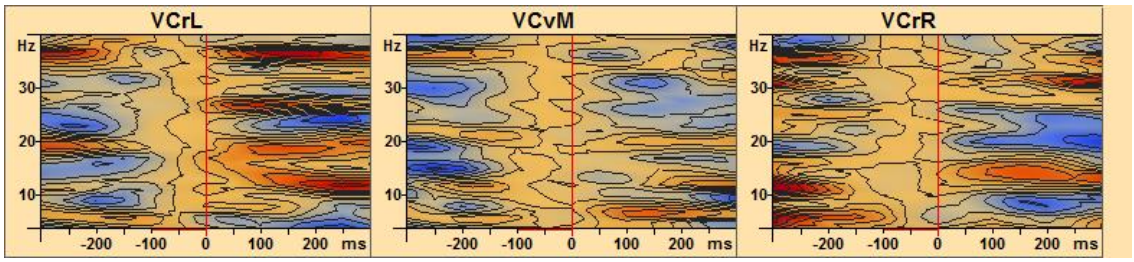

TSE maps of the combined looming condition across brain regions VCrL, VCvM, and VCrR in 12-month-old preterm infants. Induced desynchronized and induced synchronized activities are shown in blue and red contours, respectively. Epoch is from -300 ms to 300 ms and the frequency is from 4 Hz to 40 Hz.

AT

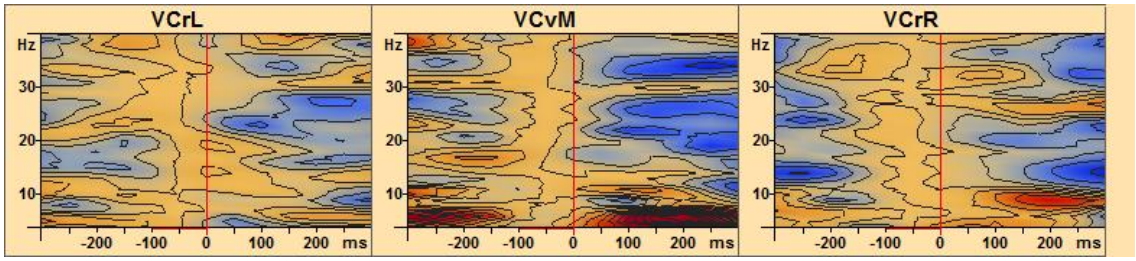

DA

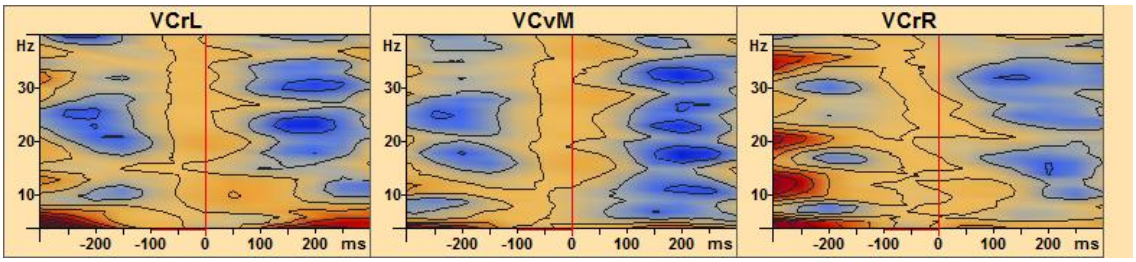

DK

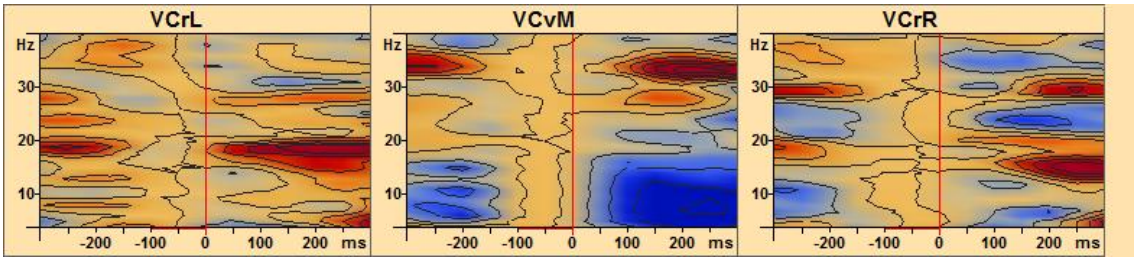

EL

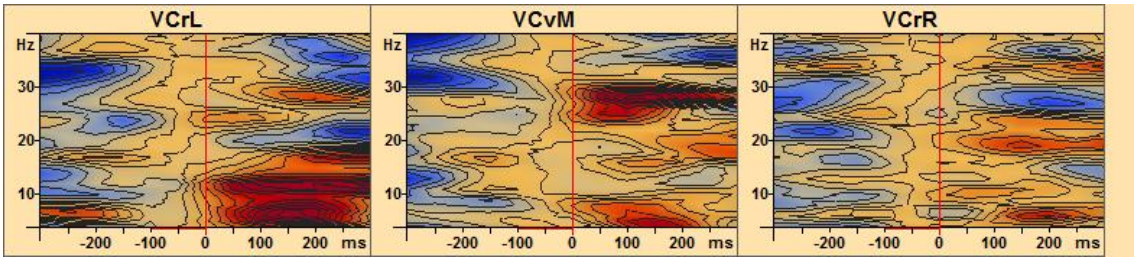

FP

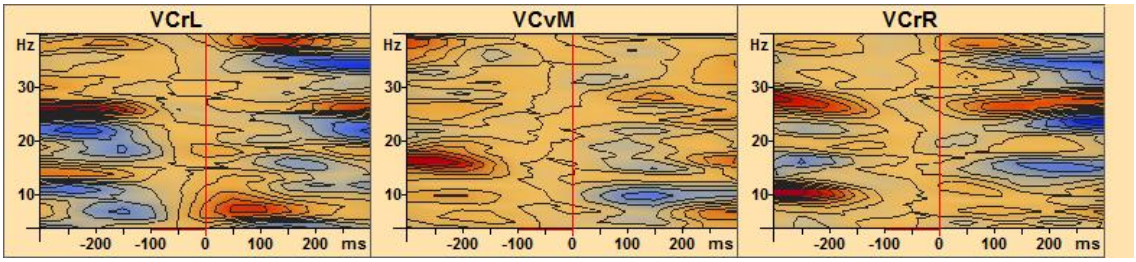

MS

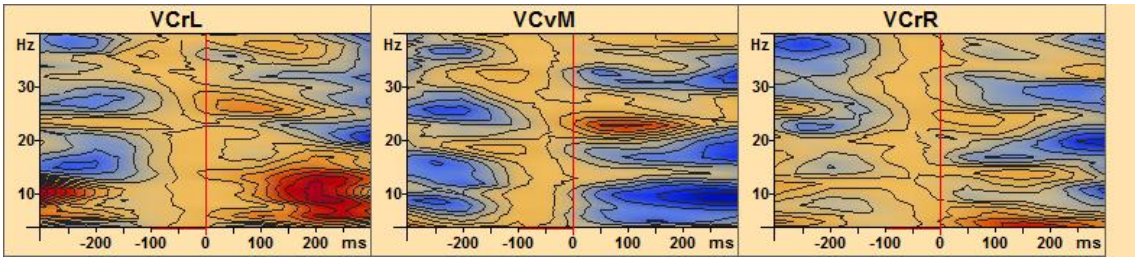

SE

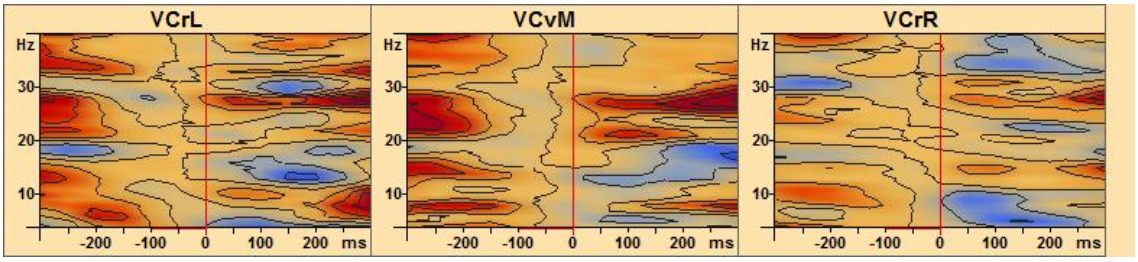

TA

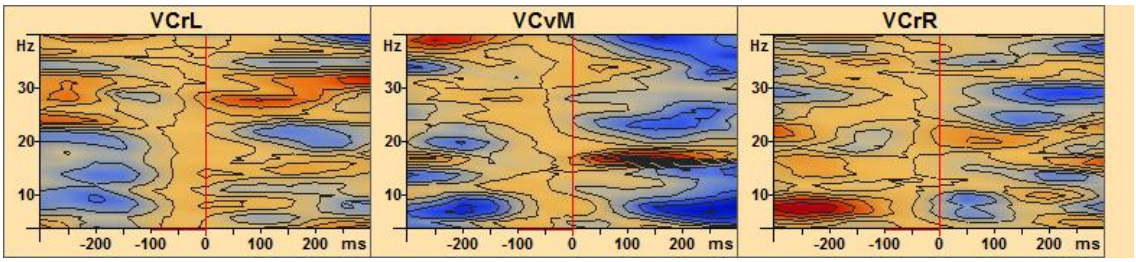
VCrL
VCvM
VCrR
Hz
30
20
10
-200
-100
0
100
200
ms

WM

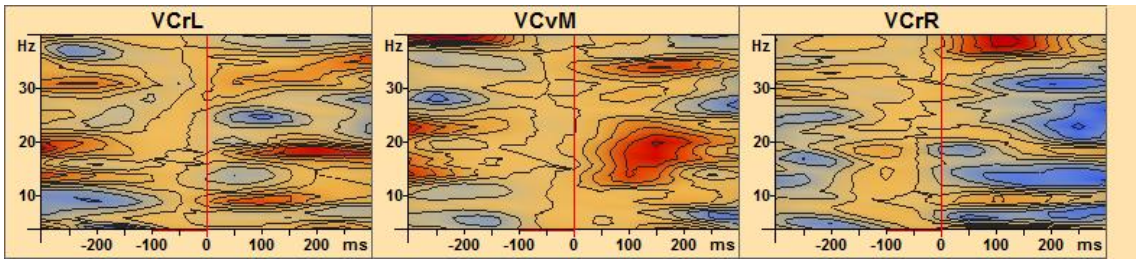
VCrL
VCvM
VCrR
Hz
30
20
10
-200
-100
0
100
200
ms